REMARKS/ARGUMENTS

Claims 1, 3, and 5-52 are pending.

Claim 1 has been amended.

Claims 2 and 4 have been cancelled.

Claims 50-52 has been added.

Support for the amendments is found in the claims and specification (e.g., page 32, 43-45, and 48, and the Examples), as originally filed.

No new matter is believed to have been added.

The claims are rejected under 35 U.S.C. 103(a) (a) over Hibino et al., *J. Chem. Soc. Faraday Trans.*, 91:1955-59 (1995) and Chandran et al., US 2002/0003085 as evidenced by Arai et al., US 6,322,910, and (b) Hibino et al., Chandran et al., Arai et al., and Diekmann et al., US 6,268,076. The rejections are traversed because the combination of the references does not describe or suggest:

(i) micro-region reaction sites,

(ii) a working electrode layer to manage oxidation-reduction reactions is formed in the upper part of the cathode, and the micro reaction regions of nanometers to a micrometer in size where the oxidation-reduction reactions take place are introduced into the working electrode layer, and the claimed working temperature is 400-700 °C (or less than 700 °C)

(iii) applied current from 5 mA to 1A or an applied voltage is from 0.5 V to 2.5 V (as in claim 50), and

(iv) a chemical reaction system which can decompose 50% of NOx at the current density of 31 mA/cm^2 or less (as in claim 51).

The claimed chemical reaction system efficiently excludes nitrogen oxides from exhaust gas containing oxygen. The system has micro reaction regions for performing oxidation and reduction reactions on a target substance introduced into a part of the chemical

reaction so that oxygen and nitrogen oxides are separated and adsorbed from an exhaust gas within the micro reaction regions, thus allowing a target substance to be efficiently processed with low electric power consumption (see page 1 of the present specification).

Rejection (a).

The Hibino et al. electrochemical cell has a simple cell structure in which a zirconia electrolyte is sandwiched between an anode and a cathode of palladium. Therefore, substantial power is consumed by pumping oxygen that coexists in a gas to be treated.

As illustrated in Fig. 3, the cell must be supplied with a *large current*, e.g., as much as 500 mA/cm^2, for even decomposing 50% of NOx.

Also, the claimed working temperature is 400-700 °C (or 400 °C to less than 700 °C) (e.g., as in the Examples of the present specification), while Hibino et al. describe that a temperature above 700 °C is required for the operation of the reactor because its large dc resistance and overpotential (page 1955, left col., second paragraph).

The claimed chemical reactor system provides a selective decomposition reaction of NOx molecules in coexisting oxygen by introducing nanoscale "micro-region reaction sites" for solving problems described in the present specification (e.g., does not require an excessive energy consumption) (see pages 3-10). The "micro reaction regions" is a structure having an interface comprising the three metal phases, an oxygen deficient part, and micro spaces (see claim 1, element (2)).

With regard to know electrochemical cells for NO decomposition, including the cell of Hibino et al., Bredikhin et al., Inonics, DOI 10.1007/s11581-008-0249-5 (2008), (submitted with this paper) describe that *without* coexisting oxygen, the decomposition was known in a cell having a structure Cathode/YSZ/Anode (as in Hibino et al.) and the decomposition of NO takes place only when all oxygen is pumped away from the near electrode area (see pages 2-3, "Traditional type of electrochemical cells for NO

decomposition"). Further, all known cathode materials used up to now for electrochemical reduction of NO show a low selectivity for NO reduction in the presence of the excess oxygen and cannot be used for practical applications (page 3, right col., last paragraph). Bredikhin et al. further describes disadvantages of previously know electrochemical cells (pages 2-3). *See also* Hamamoto et al., J. Ceramic Society of Japan, Supp., 112-1 PacRim5 Special Issue, 112(5):S1071-1074 (2004), and Aronin et al., J. Am. Ceram. Soc., 88(5):1180-1185 (2005) describing disadvantages of known cells and advantages of the claimed cell (submitted with this paper).

The Examiner has alleged that in the Hibino et al. cell, boundaries between YSZ and a cathode/anode have a metal phase of Pd electrode and some gaps formed between small particle grains. However, the Hibino et al. Pd electrodes do not comprise "an interface" comprising the metal phase and gaps because the Hibino et al. electrodes are made of Pd and, therefore, the entire Pd electrodes are "a metal phase and gaps".

The Examiner has agreed that the Hibino et al. cell does not comprise a working electrode layer and relied on Chandran et al. describing an additional Pt coating on a LMS electrode (page 1, [0010]) interpreted by the Examiner as "a working layer."

The purpose in Chandran is to form other cathodes on a cathode, in an electrochemical cell for "increasing oxygen concentration" by oxygen pumping.

A conductive porous layer 54 of Pt is formed on the cathode 52 of Fig. 3. This structure enhances permeability of the gas to be treated because of porosity, and reduces the voltage drop by suppressing resistance because of the high conductivity of a Pt cathode (see page 3).

By contrast, the "micro-reaction regions" in the claimed reaction system are micro-reaction regions where oxidation-reduction reactions of a target substance take place, and interfaces consist of a metal phase - an oxygen deficient part - micro spaces at the points of

contact between the electron conduction phase and the ion conduction phase (see claim 1). The micro-reaction regions are introduced into the cathode (see claim 3) and have a size of from a nanometer to a micrometer scale (see claim 1).

Therefore, even in the Hibino et al. single cell is supplemented with Chandran et al.'s overlapping cathodes, the combined structure provides an oxygen enrichment, while the claimed structure provides a selective decomposition of NOx.

Also, the claimed micro-reaction regions comprise a metal phase, an oxygen deficient part and micro spaces that provide NOx selective reaction sites, while the Chandran et al. structure adds a conductive porous electrode that provides an oxygen enrichment.

The effect of a selective reaction of NOx in coexisting oxygen, which is the point of the invention of the present application, is the exact opposite of the purpose of the cathodes according to Chandran et al. providing an oxygen enrichment.

Thus, Chandran et al.'s cathode cannot accomplish the goal (promoting a reaction) of the claimed reaction system.

Accordingly, the combined system of Hibino et al. and Chandran et al. AND the "micro regions", oxygen-deficient parts, nanoparticles and gaps coexisting at a nanoscale of the claimed reaction system are different. Oxygen-deficient parts, nanoparticles and gaps coexist at a nanoscale are essential for the selective decomposition reaction of NOx as micro-region reaction sites.

Moreover, the Examiner provides inconsistent arguments with regard to a combination of Hibino et al. and Chandran et al. because:

(1) The claimed system comprises (i) interfaces consisting of a metal phase of the electron conduction phase, an oxygen deficient part of the ion conduction phase and micro spaces (gaps) surrounding the contact points, wherein the interfaces are formed as micro

reaction regions, and (ii) a working electrode layer formed in the upper part of the cathode, wherein the micro reaction regions are introduced into the working layer.

(2) According to the Examiner, the Hibino et al. Pd electrode has a metal phase and gaps. The Examiner also stated that Hibino et al. do not describe the working layer. Thus, it appears that the Examiner's opinion is that Hibino et al. describe a metal phase and gaps but they are not located in the working layer. However, the metal phase and gaps of the cliamed system are a part of the micro regions, wherein the micro regions are a part of the working layer as in claim 1.

Further, even if we assume for the sake of argument that the Chandran et al. additional Pt coating (defined by the Examiner as a working layer) comprises a metal phase and gaps, the Pt coating is not forming an "interface" with an ion conduction phase but is disposed on the top of the Pd electrode which is in contact with the ion conduction phase.

In the claimed system, "the area including gap" is loaded within cathode, i.e., in the layer 2 of Figure 1.

In addition, the Examiner has asserted that the Chandran et al. cell is fully capable of reducing NOx (the goal of the claimed reaction system) (see page 3 of the Official Action). Applicants respectfully disagree.

Chandran et al. cell is for pumping oxygen which is capable of reducing NOx in the side of cathode. It is well known that NOx can be reduced at reducing side of an electrode of the electrochemical reaction cell by the teachings of Pancharatnam et al., J. Electrochem. Soc. 122, 869 (1975) (see also Bredikhin et al., Inonics, DOI 10.1007/s11581-008-0249-5 (2008), submitted with this paper describing shortcomings of the Pancharatnam et al. cell on page 2, right col.).

In the claimed system, a selective reduction of NOx under the condition of the *co-existence of oxygen* can be accomplished firstly by forming micro reaction space.

Under the condition that there is no co-existence of oxygen (as in Pancharatnam et al. and Hibino et al.), any electrochemical cell is capable of reducing NOx.

Also, the Examiner has alleged that Arai et al. describe "an oxygen deficient layer" laminated under a layer which is laminated with the addition of oxygen (col. 4, lines 55-65). The Examiner has asserted that because the Hibino et al. Pd electrodes are attached to YSZ by electroless plating without the addition of oxygen at 90 °C , an oxygen deficient layer is inherently formed at the boundary of Pd electrodes and YSZ (pages 5-6 of the Official Action). However, the entire Pd electrodes of Hibino et al. are "the oxygen deficient", because the entire Pd electrodes (not just a layer) are produced under the conditions identified by the Examiner as "oxygen deficient." Further, in the claimed system, the working layer comprises the oxygen deficient part, while, according to the Examiner, the Hibino et al. Pd electrodes comprise "an oxygen deficient layer" and the Hibino et al. cell does not comprise "a working layer."

The Examiner's arguments with regard to combining Hibino et al., Chandran et al., and Arai et al. are inconsistent.

Also, the Hibino et al. cell must be supplied with a large current, e.g., as much as 500 mA/cm^2 for decomposing 50% of NOx (fig. 3), while the claimed cell requires 31 mA/cm^2 or less for decomposing 50% of NOx, as demonstrated in the Examples of the present specification. The Hibino et al. cell is not capable of decomposing NOx at such low current density.

Thus, Hibino et al., Chandran et al., and Arai et al. do not make the claimed system obvious. Applicants request that the rejection be withdrawn.

Rejection (b).

The Examiner has alleged that functions of the Diekmann et al. barrier layer and the claimed barrier layer are the same (pages 8-9 of the OA).

In response, it is noted that the purpose of the barrier layer of the Diekmann et al. is opposite to that of claimed barrier layer, and, therefore, the Diekmann et al. is not capable of performing the function of the claimed barrier layer.

Further, Diekmann et al.'s barrier layer is capable of providing a chemical reaction in the side of cathode, while the present system is capable of reducing NOx selectively under the co-existence of oxygen.

Thus, Hibino et al., Chandran et al., and Diekmann et al. do not make the claimed system obvious. Applicants request that the rejection be withdrawn.

Claims 41 and 47 are rejected under 35 U.S.C. 112, second paragraph for lack of antecedent basis. Applicants respectfully traverse because claims 1 recites an ion conduction phase, a reduction phase, and anode an oxidation phase. However, to further clarify the invention, claim 1 has been amended. Applicants believe that claims 41 and 47 are clear.

Applicants request that the rejection be withdrawn.

A Notice of Allowance for all pending claims is requested.

Respectfully submitted,

OBLON, SPIVAK, McCLELLAND,
MAIER & NEUSTADT, P.C.
Norman F. Oblon

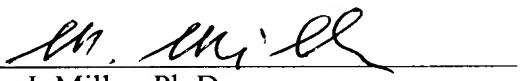

Marina I. Miller, Ph.D.
Attorney of Record
Registration No. 59,091

Customer Number
22850

Tel: (703) 413-3000
Fax: (703) 413 -2220
(OSMMN 08/07)

Ionics
DOI 10.1007/s11581-008-0249-5

REVIEW

Electrochemical reactors for NO decomposition. Basic aspects and a future

Sergey Bredikhin · Koichi Hamamoto · Yoshinobu Fujishiro · Masanobu Awano

Received: 10 April 2008 / Revised: 5 June 2008 / Accepted: 26 June 2008

Abstract The electrochemical reduction of nitric oxide in the presence of the excess oxygen was reviewed. It was shown that the selectivity and activity of the cathodes is strongly dependent on the composition and on the microstructure of the cathode material. A concept of electrochemical reactor with multilayer electro-catalytic electrode was proposed and successfully designed in Advanced Manufacturing Research Institute, National Institute of Advanced Industrial Science and Technology (AIST), Nagoya, Japan. The typical values of current efficiency in such electrochemical reactors are of the order of 10–20% at gas composition: 1,000 ppm NO and 2% O_2 balanced in He and at gas flow rate 50 ml/min. The value of current efficiency depends on the functional multi-layer electrode composition, structure, and operating temperature. Such electrochemical reactors show the value of NO/O_2 selectivity (ν_{sel}) higher than 5 ($\nu_{sel}>5$) at intermediate temperature and up to $\nu_{sel}=25$ at low temperature operation. It was shown that multilayer electro-catalytic electrode should consist at list from three main functional layers: cathode, electro-catalytic electrode, covering layer, in order to operate as an electrode with high selectivity.

Keywords Electrochemical cell · NO decomposition · Percolation · Nanosize

S. Bredikhin (✉)
Institute of Solid State Physic Russian Academy of Science,
142432 Chernogolovka, Russia
e-mail: bredikh@issp.ac.ru

K. Hamamoto · Y. Fujishiro · M. Awano
Advanced Manufacturing Research Institute, National Institute of Advanced Industrial, Science and Technology (AIST),
2266-98, Shimo-shidami, Moriyama-ku,
Nagoya 463-8687, Japan

Introduction

Striking progress has recently been made in understanding the central role of nitrogen oxide radicals, NO_x, in atmospheric processes [1]. NO_x is implicated in the formation of acid rain and tropospheric ozone (the principal toxic component of smog and a greenhouse gas) [1, 2]. The major known source of NO_x is fuel combustion and biomass burning. Air pollution by nitrogen oxides (NO_x) in combustion waste causes serious environmental problems in urban areas. The reduction of nitrogen oxide emissions has become one of the greatest challenges in environment protection [3, 4]. This is why the different methods of NO_x decomposition are intensely studied by numerous groups from academic and industrial research laboratories [5, 6].

The main activities of scientific groups working in the field of NO decomposition are concentrated on the reduction of the NO_x in the presence of NH_3, CO, H_2, or hydrocarbons. These scientific groups have been tested a large number of categories of catalysts with a different ways of NO decomposition reactions. The main directions of the research can be described as follows.

First is the selective catalytic reduction of NO with ammonia, typical for chemical industrial plants and stationary power stations [7, 8]. The main step is the reduction on NO or NO_2 to N_2 and H_2O. Generally, liquid ammonia is injected in the residual gas before the catalytic reaction takes place.

$$4NO + 4NH_3 + O_2 \rightarrow 4N_2 + 6H_2O$$
$$6NO + 4NH_3 \rightarrow 5N_2 + 6H_2O$$

Second is the catalytic reduction of NO in the presence of CO and/or hydrogen. These reactions are typical for the automotive pollution control. The use of CO or H_2 for catalytic

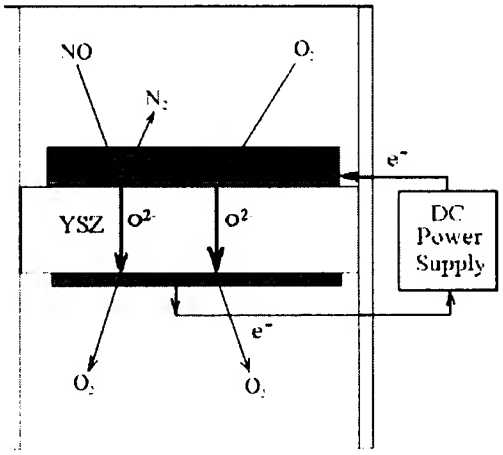

Fig. 1 Conceptual representation of the electrochemical cell for NO decomposition

reduction was one of the first possibilities investigated in view of eliminating NO from automotive exhaust gas [4, 9–12].

$$NO + CO \rightarrow CO_2 + 1/2N_2$$
$$NO + H_2 \rightarrow 1/2N_2 + H_2O$$

Third is the selective catalytic reduction of NO in the presence of hydrocarbons and more particularly methane, a method which has not yet reached industrial use but can be applied both for automotive pollution control and in various industrial plants [3, 13–18]

Fourth is the direct decomposition of NO. The decomposition of NO would represent the most attractive solution in emission control because the reaction does not require that any reactant be added to NO exhaust gas and could potentially lead to the formation of only N_2 and O_2 [6, 18–20].

The goal of this paper is to represent a fifth direction of an intense research effort focused on electrochemical cells for the reduction of NO_x gases due to the need to design an effective method for the purification of the exhaust gases from lean burn and diesel engines.

Traditional type of electrochemical cells for NO decomposition

Electrochemical cells have become an important technology, which contributes to many aspects of human life, industry, and environment. Now, it is understandable that the reduction of NO_x emission can be achieved not only by catalytic NO_x decomposition but also by electrochemical decomposition, where the removal of oxygen by a gaseous reducing reagent is replaced by the more effective electrochemical removal. Additional reducing reagents such as hydrocarbons, CO, H_2, or ammonia can lead to the production of secondary pollutants like oxygenated hydrocarbons, CO, CO_2, N_2O, or ammonia or, even, as was often reported in the past, cyanate and isocyanate compounds.

Without coexisting oxygen, the successful decomposition of NO gas into oxygen and nitrogen in a primitive electrochemical cell (Fig. 1) was first demonstrated more than 25 years ago [21, 22]. In 1975, Pancharatnam et al. [21] proposed to use, for NO gas decomposition, an electrochemical cell represented by the following cell arrangement

$$Pt(Cathode)|YSZ|Pt(Anode) \quad (1)$$

On applying a voltage to such cells, NO gas is directly reduced at the triple-phase boundary (tpb) (cathode–YSZ–gas) forming gaseous N_2 and solid-phase oxygen ions:

$$2NO + 4e^- + 2V_O(ZrO_2) \rightarrow N_2 + 2O^{2-} \ (YSZ) \quad (2)$$

Under the external voltage, the oxygen ions are transported through the solid electrolyte from cathode to anode, and gaseous O_2 is evolved at the anode.

Unfortunately, excess O_2 in the combustion exhaust gas is adsorbed and decomposed at the tpb in preference to the NO gas (Fig. 1):

$$O_2 + 4e^- + 2V_O(ZrO_2) \rightarrow 2O^{2-} \ (YSZ) \quad (3)$$

As a result, the additional ionic current, though the cell associated with the oxygen ions produced due to this unwanted reaction (Eq. 3), far exceeds the current associated with the desired reaction (Eq. 2). In 1997, Hibino [23] has shown that, at first stage, the electrochemical oxygen pumping is carried out without NO decomposition and that NO decomposition began at corresponding currents after the electrochemical oxygen pump is complete. As illustrat-

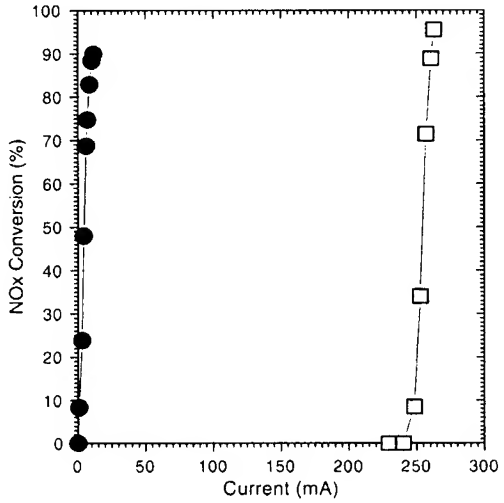

Fig. 2 Dependence of NO conversion on the value of the current passing through the two chambers cell at 1,000 ppm of NO without oxygen (*circle* curve 1) and at 2% of oxygen (*square* curve 2) in He (the balance) at gas flow rate 50 ml/min

ed in Fig. 2, the dependence of NO conversion on the value of the current passing through the two-chamber cell at 1,000 ppm of NO without oxygen (curve 1) and at 2% of oxygen (curve 2) in He (the balance) at gas flow rate 50 ml/min. It is seen that, in the presence of oxygen, the decomposition of NO take place only when all oxygen should be pumped away from the near electrode area.

Recently, many attempts to improve the properties of electrochemical cells operating in the presence of excess oxygen have been carried out by using different catalysts as the cathode material [24–28]. Walsh and Fedkiw [25] proposed substitute dense Pt electrodes to the porous platinum and to use a mixture of ionic (CeO) and electronic (Pt) conductors as a porous cathode. It is well known that substitution of dense electrode to the porous should increase gas penetration to the tpb on the surface of the YSZ-disc solid electrolyte and using of the mixture of ionic (CeO) and electronic (Pt) conductors should lead to the increase of the tpb surface area inside the cathode. As the result, both oxygen and nitrogen oxide decomposition take place in such cells and for effective NO adsorption and decomposition the tpb should be free from the adsorbed oxygen. This conclusion agrees well with a fact that the NO decomposes after the oxygen pumping is completed.

To improve the selectivity for NO gas adsorption and decomposition in the presence of the oxygen excess, Iwayama et al. [24, 29] proposed to coat Pt cathode by different metals or metal oxide. Decomposition activity was measured on metal oxide/Pd(cathode)/YSZ/Pd(anode) at 773–973 K and 3.0 V of applied voltage in a flow of 50 ml/min containing 1,000 ppm of NO and 6% of O_2 in helium. Coating of various metal oxides onto the cathode electrode greatly changed the decomposition activity; the order was $RuO_2 \gg Pt > Rh_2O_3 > Ni > none > Ag > WO_3$. The activity of the system modified by RuO_2 has been investigated as a function of the kind of electrode, the applied voltage, and the reaction temperature. The cell of RuO_2/Ag(cathode)/YSZ/Pd(anode) was found to show the most excellent activity among the cells examined.

Later [30–32], a series $La_{1-x}A_xBO_3$ perovskite were prepared and systematically evaluated for substitution of the Pt or Pd electrodes. A major target of all these researches was the promotion of NO reduction by F-center type defects in the YSZ surface or inside perovskite type cathodes [30–32].

An important characteristic of the efficiency of electrochemical cell is the value of the current efficiency coefficient (η). Current efficiency (η) can be defined from the value of the oxygen ionic current (I_{NO}) due to the oxygen from decomposed NO gas (see Eq. 2) and a total ionic current flux through the cell ($I = I_{NO} + I_{O2}$) as:

$$\eta = I_{NO}/(I_{NO} + I_{O_2}) \quad (4)$$

As illustrated, current efficiency for NO decomposition against current is plotted in Fig. 3 for LSC|YSZ|Pt and LSCP|YSZ|Pt cells [32]. It is seen that relatively high value of current efficiency, approximately 1.5%, can be obtained between 300 and 350 mA. This result shows that the unwanted reaction (Eq. 3) of oxygen gas adsorption and decomposition fare exceed the desirable reaction of NO gas adsorption and decomposition.

In 2007, Simonsen et al. [33] studied spinels with composition $CoFe_2O_4$, $NiFe_2O_4$, $CuFe_2O_4$, and Co_3O_4 as electro-catalyst for the electrochemical reduction of nitric oxide in the presence of oxygen. It was shown that spinels are active for the reduction of both nitric oxide and oxygen. The composition $CuFe_2O_4$ shows the highest activity for the reduction of nitric oxide relative to the reduction of oxygen. However, now, information was given on the characteristics of the electrochemical cells based on these cathode materials.

Kammer [34] reviewed the investigations in the field of electrochemical reduction of nitric oxide. He has shown that the electrochemical reduction of nitric oxide in several types of all solid-state electrochemical cells is possible and proposed that, in order to reduce nitric oxide in an atmosphere containing excess oxygen, further development of cathode materials are needed.

In accordance with above, we can conclude that all known cathode materials used up now for electrochemical reduction of nitric oxide show a low selectivity for NO reduction in the presence of the excess oxygen and cannot be used for practical application.

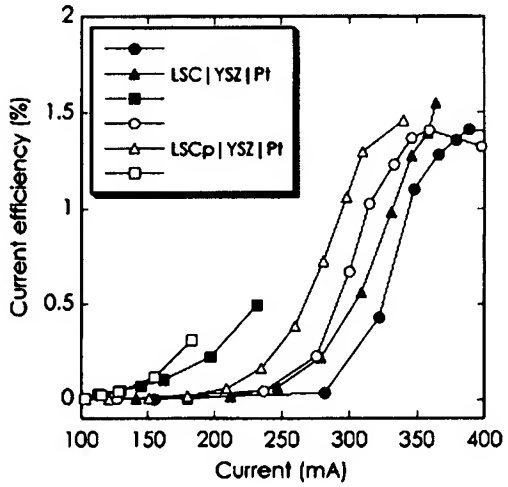

Fig. 3 Current efficiency vs. current curves of LSC u YSZ u Pt and LSPC u YSZ u Pt electrochemical cells between 600 and 800 °C (*filled circle*, *empty circle*, 800 °C; *filled triangle*, *empty triangle* 700 °C; *filled square*, *empty square* 600 °C)

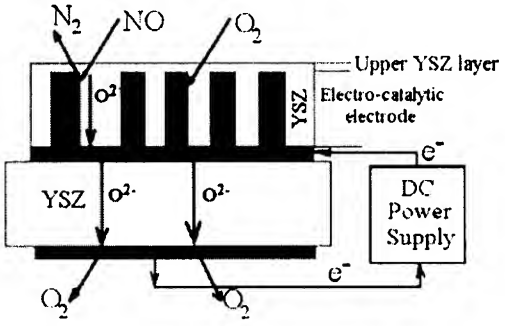

Fig. 4 Conceptual representation of the electrochemical cell with multilayer electro-catalytic electrode

Electrochemical reactors with multi-layer functional electrode

To solve the problem of effective electrochemical reduction of nitric oxide in the presence of the excess oxygen Bredikhin et al. [35–37] proposed the concept of artificially designed multilayer structure, which should operate as an electrode with high selectivity. At present time, a new type of electrochemical reactor with a functional multi-layer electrode has been successfully designed in the National Institute of Advanced Industrial Science and Technology (AIST), Nagoya, Japan [37, 38]. The typical values of current efficiency in such electrochemical reactors are of the order of 10–20% at gas composition: 1,000 ppm NO and 2% O_2 balanced in He and at gas flow rate 50 ml/min. The value of current efficiency depends on the functional multi-layer electrode composition, structure, and operating temperature. Such electrochemical reactors show the value of NO selectivity (ν_{sel}) with respect to oxygen gas molecules $\nu_{sel}>5$. This means that the probability for NO gas molecules to be adsorbed and decomposed is at least five times higher than for oxygen gas molecules.

The arrangement of the electrochemical reactor with a functional multi-layer electrode is illustrated schematically in Fig. 4. An YSZ disc with a thickness of 500 μm and a diameter of 20 mm was used as the solid electrolyte. The composite Pt(55 vol.%)–YSZ(45 vol.%) paste was screen-printed with an area of 1.77 cm^2 on one surface of the YSZ disk as the cathode and then calcined at 1,673 K for 1 h to produce a dense Pt(55 vol.%)–YSZ(45 vol.%) composite with a thickness of about 3 μm and diameter of 15 mm [38]. A dense Pt collector was connected with a cathode. The NiO–YSZ paste was screen-printed with an area of 2 cm^2 over the cathode and sintered at 1,773 K for 4 h to produce a nanoporous NiO–YSZ electro-catalytic electrode with a diameter of 16 mm and a thickness of about 5–6 μm [39–42]. The nanoporous YSZ layer with a thickness of about 2 μm was deposited over the electro-catalytic electrode as a covering layer [37]. The commercial TR-7070 (Pt–YSZ) paste was screen-printed with an area of 1.77 cm^2 on to the other surface of the YSZ disk as the anode and then calcined at 1,473 K for 1 h. Platinum mesh and wire were attached to the cathode and the anode for connection with the power supply unit.

The electrochemical reactor was set in a quartz house and connected to a potensio-galvanostat (SI1267 and 1255B, Solartron). The applied voltage and current dependence of NO decomposition behavior was investigated. The range of the applied voltage to the electrochemical cell was from 0 to 3 V. The electrochemical decomposition of NO was carried out at 573–873 K by passing a mixed gas of 500–1,000 ppm of NO and 2–10% of O_2 in He (balance) at a flow rate ν=50 ml/min. The concentrations of NO and of N_2 in the outlet gas ($[NO]_{out}$) were monitored using an on-line NO_x (NO, NO_2, and N_2O) gas analyzer (Best Instruments BCL-100uH, BCU-100uH) and a gas chromatograph (Chrompack Micro-GC CP 2002), respectively.

Bredikhin et al. [37, 38, 42] and Hamamoto et al. [43, 44] have shown that electrochemical reactors with multi-layer electro-catalytic electrode effectively operate even at low concentration of NO_x (300–500 ppm) and at the high concentration of oxygen (10%). From Fig. 5, it is seen that the efficiency of NO decomposition by electrochemical reactors with the functional multi-layer electrode far exceeds the efficiency of the traditional type of electrochemical cells.

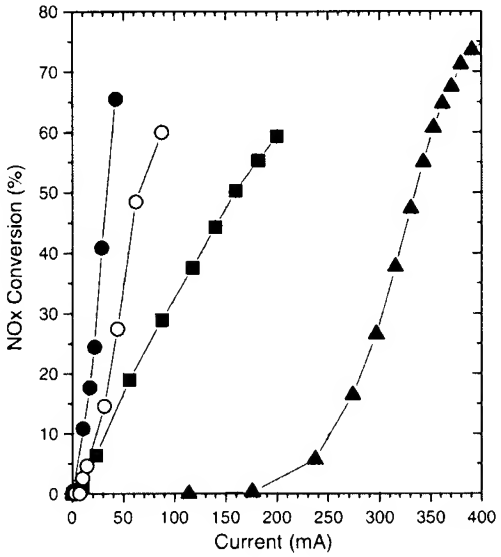

Fig. 5 The dependence of NO conversion on the value of the current for electrochemical reactors with functional multi-layer electrodes (*filled circle* 2% and *empty circle* 10% of oxygen) and for a reactor with a monolayer electro-catalytic electrode (*filled square* 2% of oxygen) and a traditional type of electrochemical cell with Pt-YSZ types of cathode (*filled triangle* 2% of oxygen)

Microstructure and properties of functional layers of multi-layer electrode

The electrochemical reactors for selective NO_x decomposition can be represented by the following reactor arrangements:

(Covering layer|Electro – catalytic electrode|Cathode)

× |YSZ|(Anode) (5a)

(Covering layer|Cathode|Electro – catalytic electrode)

× |YSZ|(Anode) (5b)

Let us consider in detail the arrangement of the electrochemical reactor with a functional multi-layer electrode and the properties of each functional layer. The cross-section view of the functional multi-layer electrode is shown in Fig. 6.

The cathode is a dense Pt(55 vol.%)–YSZ(45 vol.%) composite with a thickness of about 2–3 μm. The nanoporous NiO–YSZ electro-catalytic electrode with a thickness of about 6–8 μm was deposited over the cathode. The porous YSZ layer with a thickness of about 2–3 μm was deposited over the cathode. It is seen that the multi-layer electrode consists three main functional layers: (1) cathode, (2) electro-catalytic electrode, and (3) covering layer.

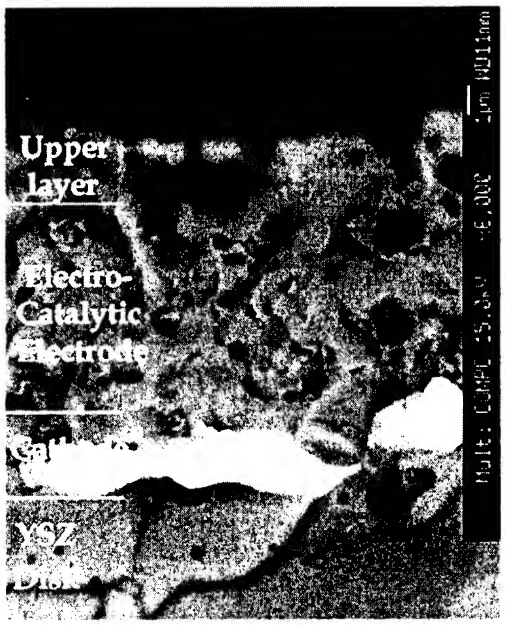

Fig. 6 The cross-section view of the multi-layer electro-catalytic electrode

Microstructure and the properties of composite cathode

The external voltage in the electrochemical reactor with a functional multi-layer electrode is applied between the cathode and anode. This voltage leads to the polarization of the YSZ disk and to the generation of a high concentration of oxygen vacancies in the near cathode region (Fig. 4). Due to the gradient in the concentration of the oxygen ions between the near-cathode region of the YSZ disk and the electro-catalytic electrode, diffusion of oxygen ions from the electro-catalytic electrode to the YSZ disk takes place. Since the oxygen ions are a charged species, their diffusion from the electro-catalytic electrode to the YSZ disk leads to an equal flux of electrons from the cathode to the electro-catalytic electrode [39–42]. As a result of electroneutrality, a decrease in the flux of the electrons should lead to the same decrease in the flux of the oxygen ions, and the diffusion of oxygen ions should be stopped when the transport of electrons is blocked. In accordance with this consideration, we can conclude that, for effective reactor operation, the cathode should be an electronic and oxygen ionic current conductor with high electronic conductivity along the cathode plane and high oxygen ionic conductivity from the electro-catalytic electrode through the cathode to the YSZ solid electrolyte [38].

In 2004, Awano et al. [37] studied the correlation between the efficiency of NO decomposition by electrochemical cells with electro-catalytic electrode and the YSZ-Pt cathode compositions. In this study, Awano et al. [37] examined $YSZ_{(X)}$–$Pt_{(1-X)}$ composite as a cathode for electrochemical cells with a functional multilayer electrode. Electrochemical cells with electro-catalytic electrode and $YSZ_{(X)}$–$Pt_{(1-X)}$ composite cathode with 0, 15.0, 24.8, 35.2, 45.4, 49.9, 55.0, and 64 vol.% of YSZ were obtained. Investigation of the current–voltage (I-V) characteristics of the electrochemical cells with multilayer electrode has shown a strong dependence on the composition of the YSZ–Pt cathode [37]. The best performance was observed for electrochemical cells with YSZ volume contents slightly lower than 50 vol.%. To investigate this behavior in detail, the value of the current has been plotted as a function of the volume content of YSZ in the YSZ–Pt composite cathode for different values of the electrochemical cell operating voltage. These experimental data are shown in Fig. 7. From this figure, it is seen that an increase of the YSZ content from 0% to 49.9% leads to a four to five times increase in the value of the current through the cell at the same value of the cell operating voltage. At the same time, a small change in the composition of the YSZ–Pt cathode by increasing the YSZ content to more than 50 vol.% leads to an abrupt decrease in the value of the current passed through the cells (Fig. 7), and at 55 vol.% of YSZ, current higher than 1 mA

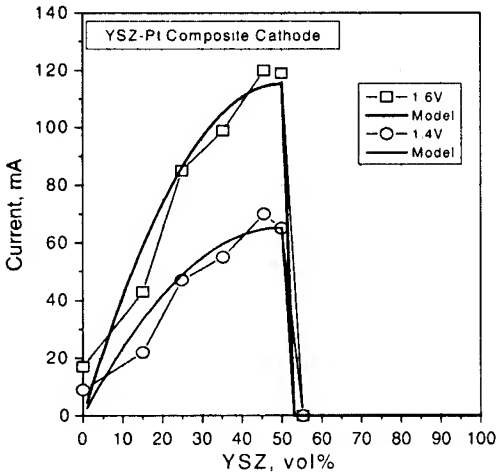

Fig. 7 The experimental dependence of the current on the volume fraction of YSZ in the YSZ-Pt cathode for applied voltages of 1.4 and 1.6 V, and comparison with calculated dependencies

cannot be passed even at applied voltages to the cells of more than 3 V. To describe these phenomena, let us consider the processes of electronic and ionic transport through the composite YSZ–Pt cathode. The geometry of the employed electrochemical cell means that electronic transport take place along the cathode through the network of Pt particles and from the cathode through the three-dimensional network of pathways from NiO or Ni particles to three-phase boundary (TPB) on the surface of the pores inside the electro-catalytic electrode. Oxygen ionic transport takes place perpendicular to the YSZ–Pt cathode plane from the electro-catalytic electrode through the network of YSZ particles to the YSZ disk.

Figure 8 shows the cross-sectional view of the electrochemical cells for different YSZ–Pt cathode compositions. It is seen that the addition of YSZ particles to the cathode leads to the formation of oxygen-conducting YSZ bridges through the electronically conducting Pt cathode and that the number of such bridges increases with an increasing amount of YSZ in the cathode. From Fig. 8, it is seen that the average size of the electronically insulating (YSZ) particles and electronically conducting (Pt) particles are of the order of 2–3 mm and are the same as the thickness of the cathode layers. These observations give us the possibility to conclude that the YSZ–Pt cathode is a quasi two-dimensional system and that the two-dimensional percolation model can be used to describe the electronic conductivity along the plane of the YSZ–Pt cathode. In accordance with this model, a sharp transition in electronic conductivity along the cathode should be observed at 50 vol.% of the electronically conducting Pt phase [37]. This means that the electronically conducting Pt phase is continuous when the volume fraction of the electronically insulating YSZ phase is less than 50 vol.%, and the Pt phase becomes disconnected when the volume fraction of insulating YSZ phase is greater that 50 vol.%. This two-dimensional percolation model prediction is in good agreement with the experimentally observed sharp threshold of the value of the current through the electrochemical cell as a function of the volume content of YSZ in the YSZ–Pt composite cathode (Fig. 7) [37].

As follows from Figs. 7 and 8, an increase of the YSZ content leads to an increase in the oxygen ionic current through the cell at a given value of the applied external voltage. At the same time, when the YSZ content exceeds the percolation threshold (50 vol.%), the Pt phase becomes disconnected, and the flux of electrons from the cathode to the electro-catalytic electrode is blocked. As a result, the oxygen ionic diffusion from the electro-catalytic electrode to the YSZ disk is stopped. In accordance with the above results, it is seen that the most critical place for oxygen ion diffusion from the electro-catalytic electrode to the YSZ disk is the oxygen transport through the composite YSZ–Pt cathode and that compositions with a volume fraction of YSZ slightly lower than the two-dimensional percolation threshold (1/2) should have the highest efficiency for charge transport through the electrochemical cell [37].

Electro-catalytic electrode

Peculiarity of ambipolar conductivity of the electro-catalytic electrode

The external voltage (V_0) in the electrochemical reactor is applied between the cathode and the anode (Fig. 4), and the voltage drop is equal to the sum of the polarizing voltage (V_{pol}) and to the Ohms voltage ($V_{Ohm}=R_{YSZ} \times I_{ox}$) drop through the YSZ disk

$$V_0=V_{pol}+V_{Ohm}=V_{pol}+R_{YSZ} \times I_{ox}, \quad (6)$$

where R_{YSZ} is the resistance of the YSZ disk and I_{ox} is the value of oxygen ionic current through the cell. The formation of the gradient in the concentration of the oxygen ions in the YSZ disc under the DC polarization voltage V_{pol} can be described in accordance with the well-known equation [44–47]

$$\mu_{cathode} = \mu_{anode} + 2e \times V_{pol}$$
$$= \mu_0 + 1/2kT \ln(P_{O_2}/P_0) + 2e \times V_{pol}, \quad (7)$$

where μ_0 and P_0 are standard values and where the chemical potential of the oxygen at the surface of the electro-catalytic electrode (μ_{CE}) and in the anode region of YSZ disc (μ_{anode}) is fixed by the oxygen gas pressure (P_{O_2}) ($\mu_{CE} = \mu_{anode} = \mu_0 + 1/2kT \ln(P_{O_2}/P_0)$). Then, the differ-

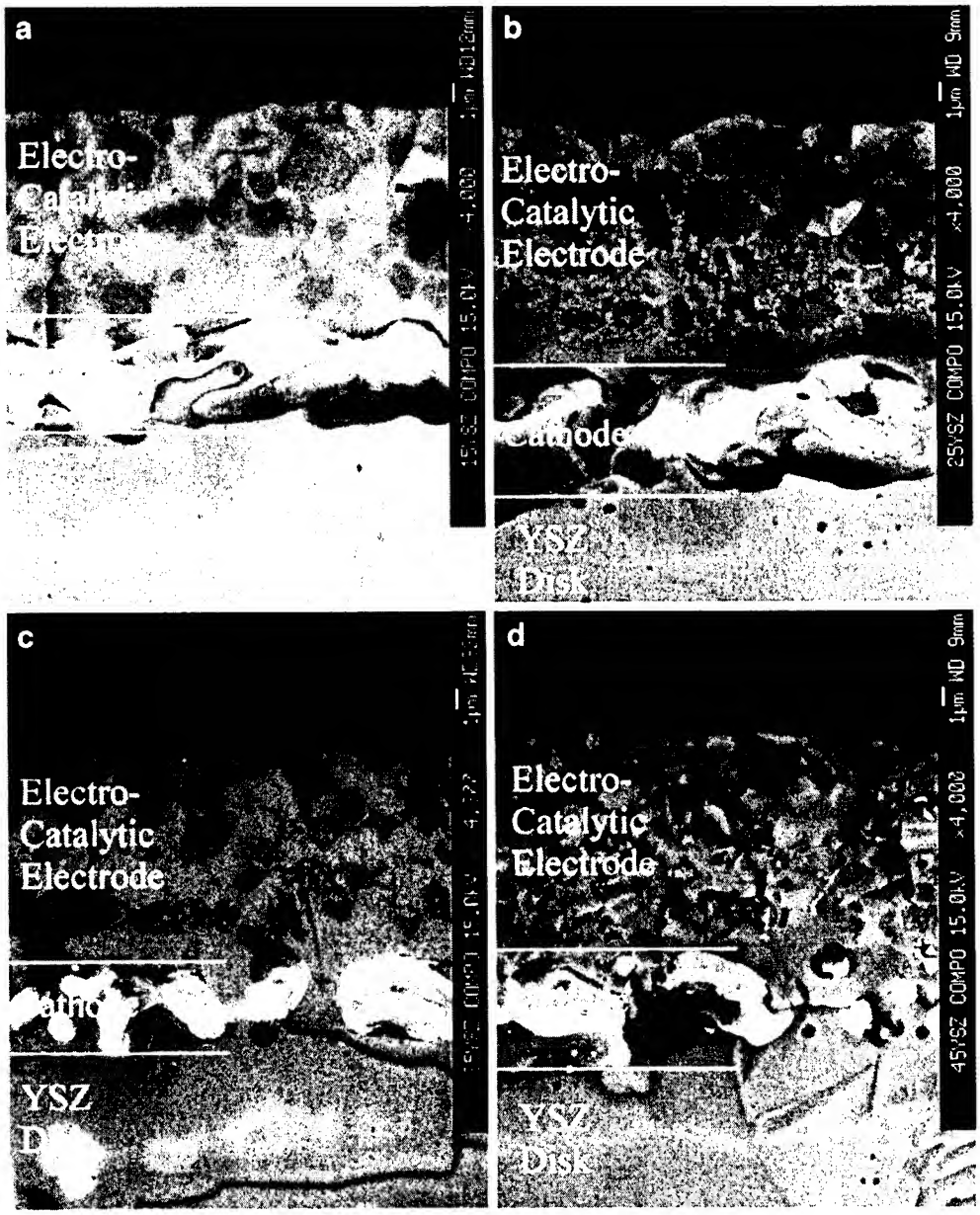

Fig. 8 SEM images of the cross-section of the multi-layer cells with different YSZ-Pt cathode compositions (**a** 15 vol. % of YSZ, **b** 25 vol.% of YSZ, **c** 35 vol.% of YSZ, **d** 45 vol.% of YSZ)

ence in the chemical potential between the near cathode region and the surface of the electro-catalytic electrode should result in the Nernst potential formation ($\Delta\phi$) through the electro-catalytic electrode

$$\Delta\phi = V_{\text{pol}} = (V_0 - R_{\text{YSZ}} \times I_{\text{ox}}) \tag{8}$$

The value of the oxygen ionic current through the electro-catalytic electrode depends on the value of the Nernst potential and on the value of the electro-catalytic electrode ambipolar conductivity (σ_{amb}) as

$$I_{\text{ox}} = \Delta\phi \times \sigma_{\text{amb}} \tag{9}$$

As follows from Eqs. 8 and 9, the value of ionic current through the electrochemical cell depends on the value of ambipolar conductivity of electro-catalytic electrode (σ_{amb}) and on the value of oxygen ionic conductivity (R_{YSZ}) of YSZ disc as

$$I_{\text{ox}} = (V_0 \times \sigma_{\text{amb}})/(1 + R_{\text{YSZ}} \times \sigma_{\text{amb}}). \tag{10}$$

It is seen that when $R_{\text{YSZ}} \times \sigma_{\text{amb}} < 1$, there is a linear dependence between ionic current through the cell and the value of ambipolar conductivity

$$I_{\text{ox}} \approx (V_0 \times \sigma_{\text{amb}}). \tag{11}$$

In 2001, Bredikhin et al. [35, 36, 48] has shown that, for electrochemical cells with nanoporous electro-catalytic electrode, there is a linear dependence between the value

of NO conversion (ΔNO) and value of oxygen ionic current passed through the cell

$$\Delta\mathrm{NO} = (1/(F \times \nu \times n)) \times \eta \times I_{\mathrm{ox}}, \quad (12)$$

where n=2 is the charge of the oxygen ions, F is a Faraday constant, ν is a total gas flow rate, and η is current efficiency. From Eqs. 11 and 12, it is follows that the rate of NO decomposition depends on the external voltage applied to the cell and on the value of ambipolar conductivity as

$$\Delta\mathrm{NO} = (1/(F \times \nu \times n)) \times \eta \times V_0 \times \sigma_{\mathrm{amb}} \quad (13)$$

It is obvious that, for optimization of the electrochemical cell for NO decomposition, it is necessary to design the cell with the highest value of the ambipolar conductivity. To analyze the specific features of the ambipolar conductivity of the NiO–YSZ composite electrode the calculated value of σ_{amb} (see Eq. 11) has been plotted as a function of the volume content of NiO in the NiO–YSZ composite electrode. These data are shown in Fig. 9. It is seen that, when the external voltage is higher then 1.5 V, the two percolation transitions of electronic and ionic conductivities lead to a composition range from 1/3 to 2/3, in which the ambipolar conductivity is much higher than those in the other regions. This suggests that, in order to achieve high value of ambipolar conductivity, the volume fractions of each phase have to be within 1/3~2/3, and external voltage should be higher then 1.5 V. It should be noted that in the composition range from 1/3 to 2/3, the value of ambipolar conductivity increases with increasing of the voltage applied to the cell. As an illustration, Fig. 10 shows the dependence of the value of the ambipolar conductivity on the voltage for two NiO–YSZ composite electrodes with NiO volume content 82.5% and 35%.

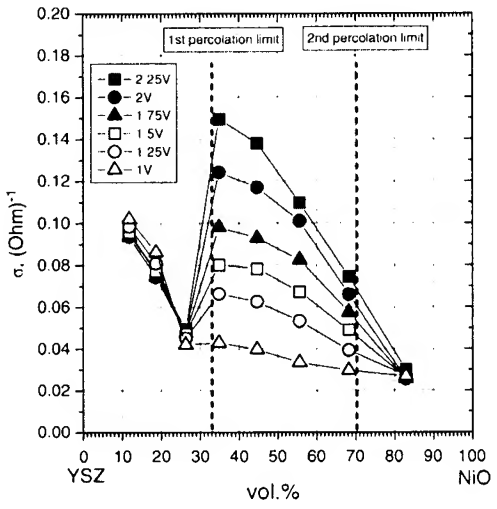

Fig. 9 The dependence of the value of the ambipolar conductivity on the volume fraction of NiO in Ni YSZ electro-catalytic electrode

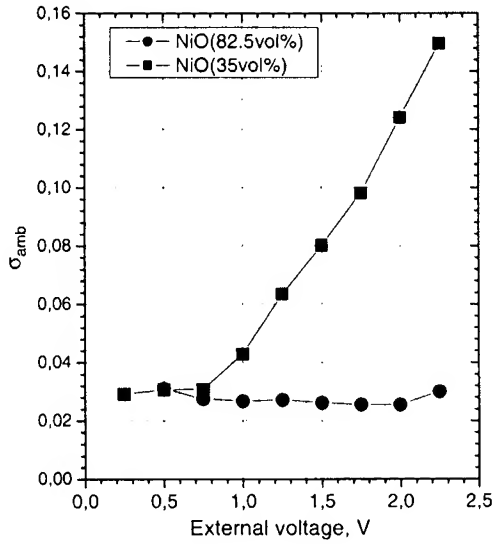

Fig. 10 The dependence of the value of the ambipolar conductivity on the cell operating voltage for two NiO YSZ composite electrodes with NiO volume content 82.5% and 35%

From Figs. 9 and 10, it is seen that for the composition range from 1/3 to 2/3 the application of external voltage leads to six to ten times increase of the value of ambipolar conductivity. Such unusual dependence of the value of conductivity on the applied voltage shows that change of the chemical composition of NiO–YSZ electro-catalytic electrode takes place under the cell operation.

Reduction–oxidation processes and the structure of the electro-catalytic electrode

The distinguishing feature of such reactors is the artificial nanostructure formed in the NiO/YSZ interface of the electro-catalytic electrode under operation. The essential changes occur in the interfacial boundary region between NiO and YSZ grains. After the electrochemical cell

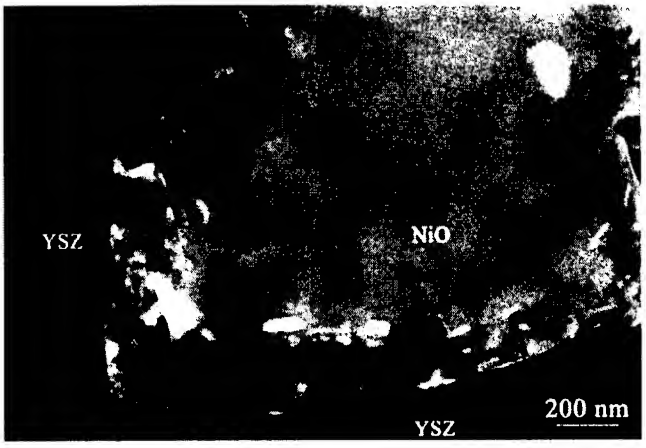

Fig. 11 Interfacial boundary between YSZ and NiO grains of the sample after cell operation

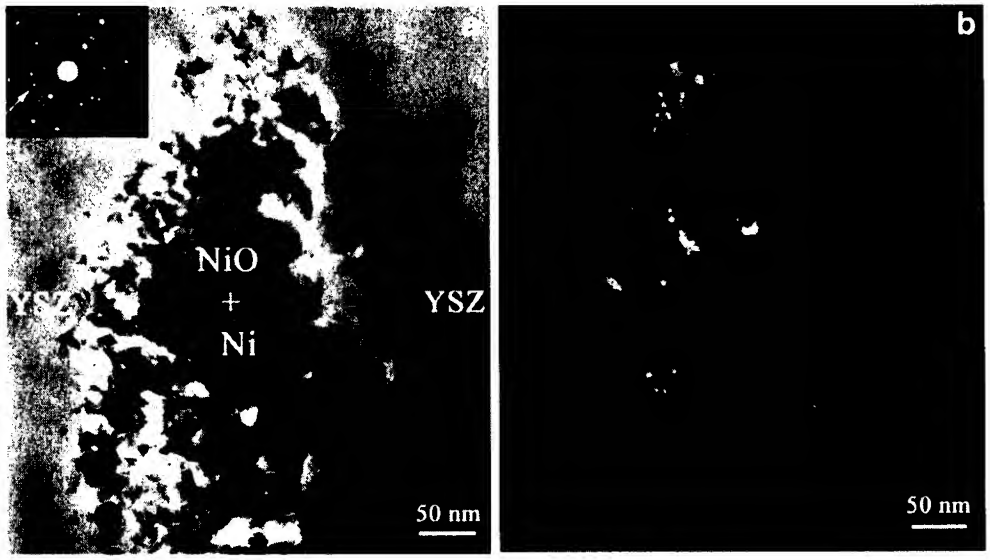

Fig. 12 Bright field TEM image (**a**) and dark field TEM images (**b**) of new NiO and Ni grains zone devoured "old" NiO grain

operation for 22 h at a cell voltage lower than 2.2 V they are as follows [39]:

1. New grains nucleate and grow in the pore zone of NiO near-boundary regions. The zone of new grains spreads into the depth of the NiO grain (Fig. 11). In some cases, this zone of new grains devours "old" NiO grain completely (Fig. 12a, b). The electron diffraction patterns from these regions contain ring reflections of Ni in addition to NiO reflections [39]. The size of Ni grains is 5–20 nm, and they are seen in the dark field electron microscopy image (Fig. 12b). This image was obtained in the reflection marked by the arrow in the electron diffraction pattern (Fig. 12a, insert). The new grains are both Ni and NiO phases.
2. In the region with new NiO grains, the pores are located both in the interfacial vicinity and before the front of new growing grains. Sometimes, small NiO grains are surrounded by the pores on all sides. Separate pores are also observed in the region of new grains, located between the new grains (Fig. 11). The high-resolution electron microscopy images of the near-boundary region of YSZ grain and small NiO grain formed during the cell operation at different magnifications are shown in Fig. 13. The size of the new NiO grains varies from 10 to 100 nm depending on the location.
3. An orientation relationship has been found to exist between the lattices of YSZ and new NiO grains:

$$(310)_{YSZ} \| (110)_{NiO}, [001]_{YSZ} \| [111]_{NiO}$$

The presence of the orientation relationship between the lattices of YSZ and NiO grains indicates that the new NiO grains may nucleate on the YSZ grains as on the substrate, and in this case, their surface energy will decrease. This result is a direct evidence of the process of oxygen spillover from YSZ to Ni grains even in the presence of oxygen in the surrounding gas.

The distinguishing feature of the microstructure of the YSZ/(Ni–NiO) interface is the 10- to 50-nm Ni grains

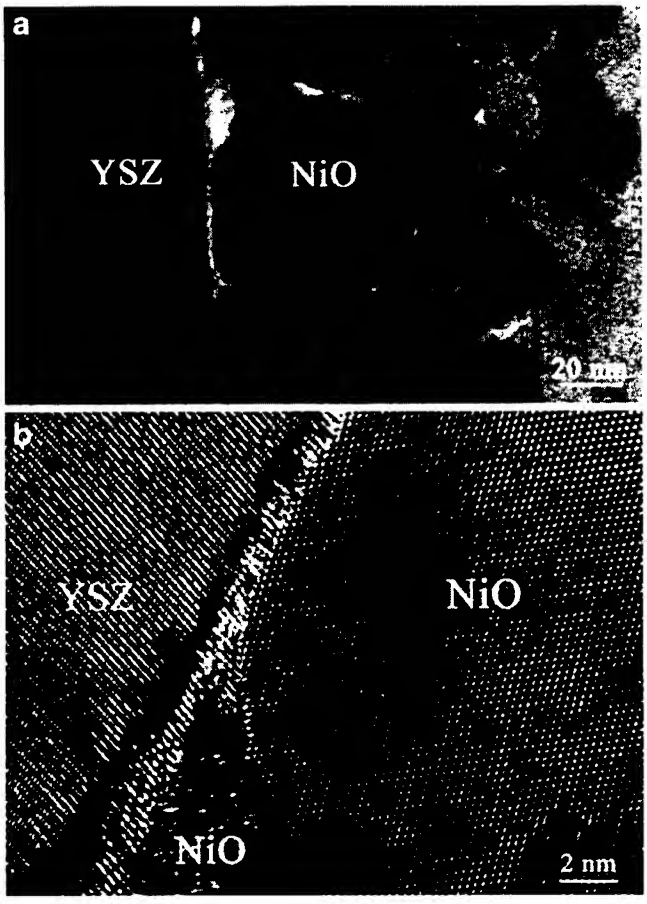

Fig. 13 HREM images of a near-boundary region of an YSZ grain and small NiO grains formed during the cell operation (**a** and **b** different magnification)

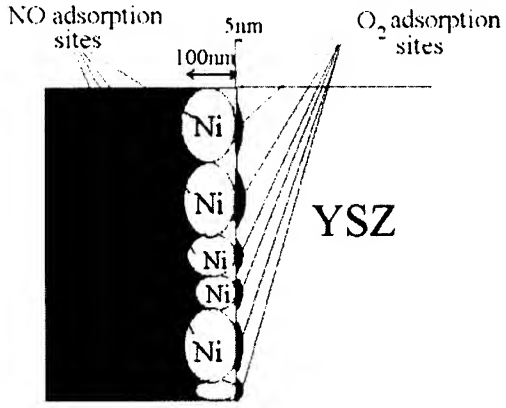

Fig. 14 Schematic representation of the microstructure of the YSZ NiO interface and of the sites for NO and oxygen gases adsorption in the self-assembled electro-catalytic electrode

reversibly produced during the reactor operation. Schematically, the microstructure of the YSZ/NiO interface reversibly produced during the cell operation is represented in Fig. 14. It is well known that adsorption and decomposition of NO_x gas molecules occurs in preference to oxygen gas molecules on Ni grain surfaces [18–20]. In addition, we should mention that rough surfaces and nanosize Ni grains are much more active for breaking of NO chemical bonds than smooth, flat surfaces [6, 19]. Based on the above results, the following reaction mechanism was proposed for NO decomposition on the nanosize Ni grains produced during the reactor operation.

$$NO + Ni \rightarrow Ni - NO \tag{14}$$

$$2Ni - NO \rightarrow 2NiO + N_2 \tag{15}$$

NO gas molecules are first chemisorbed on Ni. As a second step, the chemisorbed NO decomposes to form N_2, oxidizing Ni to NiO.

Oxygen ionic current passed though the network of YSZ particles surrounding the Ni grains. This process removed oxygen species from the electrode and permitted reactions 14 and 15 to reoccur. The regeneration reaction of the reduction of NiO to Ni takes place at the NiO/YSZ interface under the reactor operation

$$NiO + V_O(ZrO_2) + 2e \rightarrow Ni + O^2\ (ZrO_2). \tag{16}$$

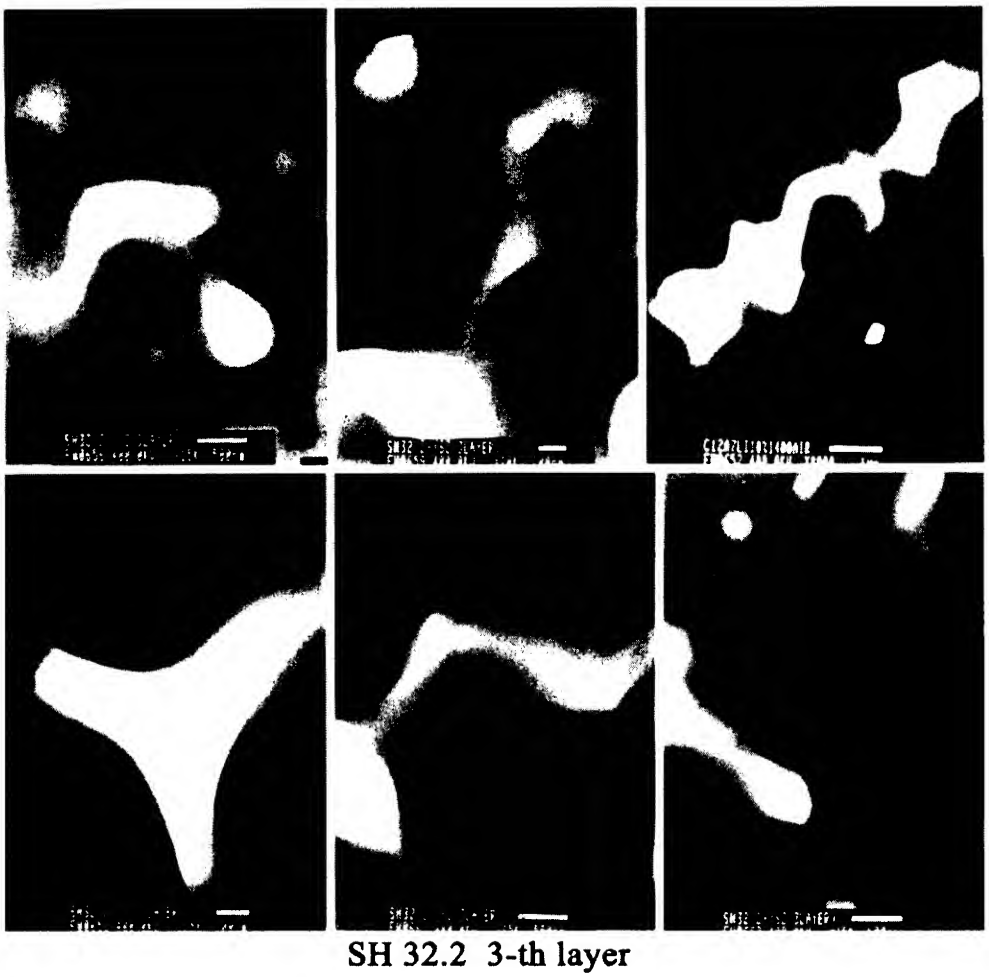

Fig. 15 TEM images of the structure of the covering YSZ layer sintered at 1450 °C

Therefore, the reduction of NiO grains into Ni grains and the oxidation of Ni grains into NiO take place continuously during reactor operation. As a result, the catalytic activity for NO decomposition is independent of the operation time.

At the same time, oxygen gas molecules have a preference for adsorption by F-type centers on the surface of YSZ.

$$O_2+4e^-+2V_O(ZrO_2) \rightarrow 2O^{2-}(ZrO_2) \quad (17)$$

From this consideration, it follows that under the reactor operation adsorption and decomposition of NO and O_2 gas molecules occur on the surface of Ni grains and by F-centers on the surface of YSZ grains, respectively. The design of an electrochemically assembled electrode with two kinds of active sites provides a way to suppress the unwanted reaction of oxygen gas adsorption (Eq. 17) and to increase the desirable reaction of NO gas decomposition (Eqs. 14, 15).

Covering layer

The deposition of a thin (2–3 nm) covering YSZ layer leads to a suppression of the oxygen adsorption and decomposition. Additionally, the deposition of the covering layer leads to an increase of the amount of nanosize Ni grains located in the near interface boundary porous region between the grains of NiO and YSZ. As a result, electrochemical reactors with the functional multilayer electrode show much better selectivity for NO gas decomposition even with respect to the electrochemical cells with electro-catalytic electrode but without a covering layer.

To optimize the characteristics of the electrochemical cells with multi-layer electrode, we have carried out the investigations of rate of NO_x decomposition depending of the upper layer microstructure. Our investigations has shown that the best characteristics of the cells for selective NO decomposition can be reached for the electrochemical cells with the thin upper YSZ layer (2–3 μm) sintered at temperature 1,450 °C.

The transmission electron microscopy investigations of the upper layer and of the electro-catalytic electrode were carried out on a Jeol 4000 FX microscope. Foils for the electron microscopy investigations were prepared by mechanical polishing followed by ion milling. The structure of the upper YSZ layer sintered at temperature 1,450 °C is shown in Fig. 15. This figure shows some typical microstructures of the upper layer. It is seen that upper layer is porous and that the pores form channels with a size of 200–500 nm, or they have ellipsoidal shape with a size 50–100 nm. The structure of the electro-catalytic electrode in the electrochemical cell with multi-layer electrode is shown in Fig. 16.

This figure shows a typical structure of electro-catalytic electrode after the cell operation. Data of chemical composition of this structure obtained by energy dispersive spectroscopy (EDS) method are also displayed in the same figure. From Fig. 16, it is seen that the structure consists of NiO, Ni, and YSZ grains. The Ni grins are located in the near-interface boundary porous region between the grains of NiO and YSZ. From the above consideration, it follows that this structure is the same as a structure of the field-quenched electro-catalytic electrode in the cells without upper layer [39, 43]. It is obvious that deposition of the upper layer leads to suppressing of the oxygen gas adsorption and to an increase of the concentration of the oxygen vacancies in the YSZ grains. As the result, both the rate of the reduction of the NiO to Ni and of the amount of new Ni grains increase in the YSZ/(Ni–NiO) interface region. Therefore, the electrochemical cells with multi-layer electrode should show a much higher selectivity for NO_x gas decomposition in the presence of excess oxygen than all known cells.

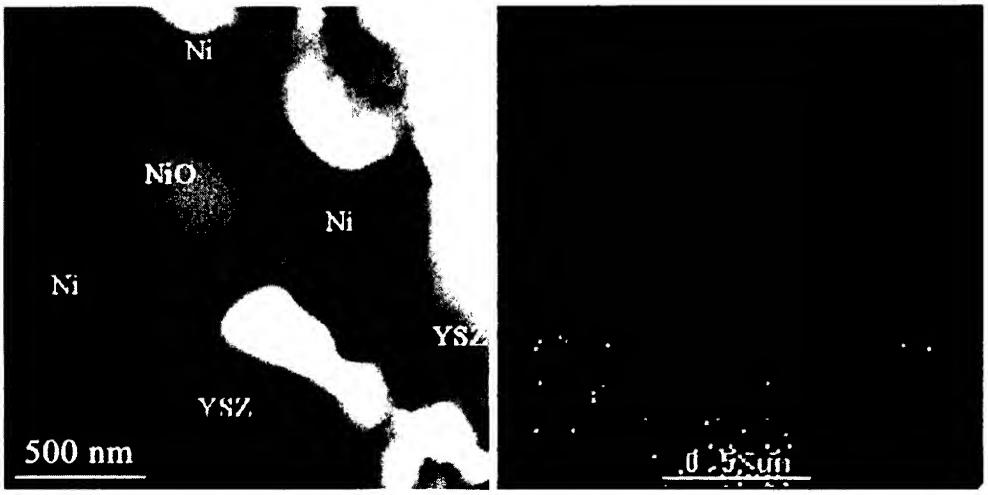

Fig. 16 TEM image of the structure of the electro-catalytic electrode (**a**) and the chemical composition of this structure obtained by EDS method (**b**)

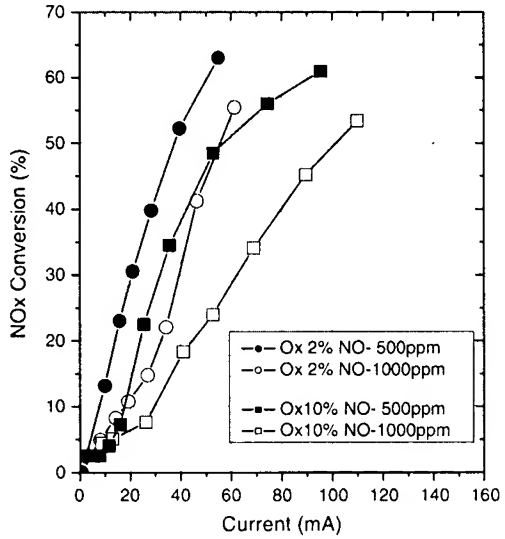

Fig. 17 The dependence of NO conversion on the value of the current for electrochemical cells with multi-layer electro-catalytic electrodes in the presence of 2% of Oxygen (*filled circle* 500 ppm and *empty circle* 1,000 ppm of NO gas) and of 10% of Oxygen (*filled square* 500 ppm and *empty square* 1,000 ppm of NO gas)

One more important advantage of the electrochemical reactor with multi-layer electrode should be discussed. Our investigations have shown that electrochemical cells with multi-layer electro-catalytic electrode effectively operate even at low concentration of NO_x (300–500 ppm) and at the high concentration of oxygen (10%) in the exhaust gas. In Fig. 17, the NO conversion is plotted as a function of the current for one compartment electrochemical cell with multi-layer electrode at different concentration of NO (500 or 1,000 ppm) and oxygen (2% or 10%) at a gas flow rate of 50 ml/min and at temperature 560 °C. From this figure, it is seen that the decrease of the NO concentration from 1,000 to 500 ppm leads to the two times decrease of the value of the current required for 30% NO decomposition for both 2% and 10% of oxygen in the gas mixture. Direct proportion between NO concentration in the exhaust gas and the value of the current required for NO decomposition confirms our proposal that the process of NO gas adsorption and decomposition is practically independent of the oxygen gas adsorption and decomposition. In addition, we should mention that increase of the oxygen content in the investigated gas from 2% to 10% at fixed NO concentration leads to the 1.5 times increase only of the value of the current required for NO decomposition. This result shows that the oxygen adsorption and decomposition in the electrochemical cells with multi-layer electrode is suppressed. In accordance with above, we can conclude that new type of electrochemical reactor with multi-layer electro-catalytic electrode can be used for effective NO decomposition even in the presence of high oxygen concentration.

The design of the self-assembled electrode with two kinds of active sites provides a way to suppress the unwanted reaction of oxygen gas adsorption and to increase many times the desirable reaction of NO gas decomposition. For the first time, an electrochemical cell with multi-layer electro-catalytic electrode for selective NO decomposition in the presence of excess oxygen (10%) operating at a low value of electrical power was designed. These results indicate that electrochemical reactors with multi-layer electro-catalytic electrode can be used for practical applications.

Intermediate and low temperature electrochemical reactors with multilayer functional electrode

In 2006, Hamamoto et al. [43, 44] proposed to use an electrochemical rector with multilayer functional electrode for intermediate temperature operation. The cell performance represented on Eq. 5b was used for intermediate temperature operation.

8YSZ (8 mol% Y_2O_3-doped ZrO_2), 10YSZ (10 mol% Y_2O_3-doped ZrO_2), and ScCeSZ (10 mol % Sc_2O_3 and 1 mol % CeO_2-doped ZrO_2) were selected as solid electrolytes. The electro-catalytic electrodes with compositions NiO–8YSZ, NiO–10YSZ and NiO–ScCeSZ (with 55 mol% of NiO) were deposited on the surface of 8YSZ, 10YSZ, and ScCeSZ solid electrolyte disks, respectively. Figure 18 shows the values of current efficiency (η) plotted as a function of applied voltage for such electrochemical reactors operated at 475 °C. The value of selectivity (ν_{sel}) of such reactors for NO gas molecules decomposition is also displayed in Fig. 18 [43]. From Fig. 18, it is seen that in electrochemical reactors with electro-catalytic electrodes the probability for NO gas molecules to be adsorbed and

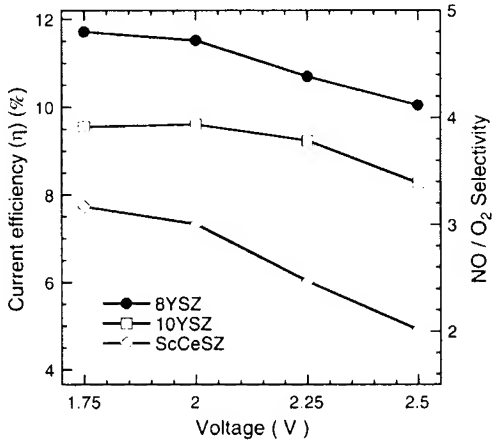

Fig. 18 Dependence of current efficiency for NO decomposition and NO/O_2 selectivity on operating voltage at 475 °C

decomposed is at least five times higher than for oxygen gas molecules.

In 2008, Hamamoto et al. [49] proposed to use an electrochemical reactor with additional NO_x adsorption layer deposited on the top of the multilayer electro-catalytic electrode. Such type of cell can be represented by following cell arrangement:

$$NO_x \text{ adsorbent}|(\text{Covering layer}|\text{Cathode}|\text{Electro} - \text{catalytic electrode})|\text{YSZ}|(\text{Anode}) \quad (18)$$

The authors [49] tested three systems that are generally used as NO_x adsorber catalyst. The $Pt/K/Al_2O_3$, $Pt/Na/Al_2O_3$ and $Pt/Cs/Al_2O_3$ adsorbents were prepared from a Al_2O_3 (Merck, p.a., specific surface area=10 $m^2\ g^{-1}$) support suspension in water, to which a solution containing KNO_3 ($NaNO_3$, $CsNO_3$) and with aqueous solutions of platinum nitrate [$Pt(NO_3)_2$] was added, in order to obtain a load of 10 wt.% of K (Na and Cs) and 3 wt.% of Pt. The mixture was heated while being vigorously stirred until a paste was achieved, which was dried in an oven for 24 h at 200 °C and crushed and calcined at 600 °C for 2 h.

To clarify the capability of a NO_x adsorption layer on the multilayer cathode, Hamamoto et al. [49] carried out the NO_x decomposition measurements of the YSZ-based cells with and without a NO_x adsorbent at a fixed operating voltage, U=2.5 V, on the cells under various O_2 concentrations at 500 °C by passing a mixed gas with 1,000 ppm of NO in He through the cell at a gas flow rate of 200 ml/min (Fig. 19). As a result, NOX adsorption layers have improved the NOX decomposition properties though the current values of each cell were almost the same.

From Fig. 19, it is seen that the values of current efficiency (η) for electrochemical reactor with the Pt/K/Al_2O_3 adsorbent are four to five times higher compared with the reactor without adsorbent. The values of current efficiency in such reactors increase up to 20% and the values of the NO/O_2 selectivity up to 25 (Fig. 20). Additionally, we should mention that such electrochemical reactors effectively decompose NO_x even at low temperature range (<300 °C).

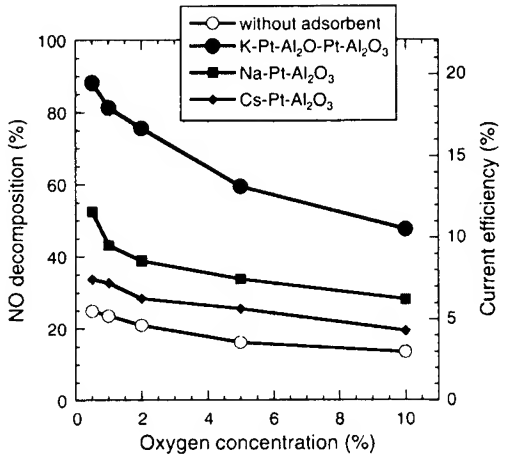

Fig. 19 Dependence of NO decomposition and of the value of current efficiency on the O_2 concentrations for the YSZ based electrochemical reactor with and without a NO_x adsorbent at 500 °C

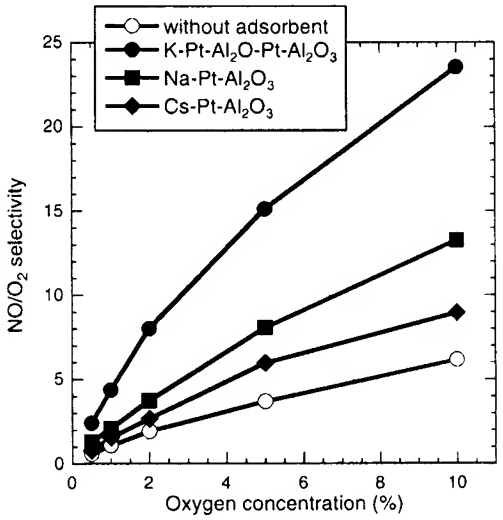

Fig. 20 Dependence of NO/O_2 selectivity on the O_2 concentrations for the YSZ-based electrochemical reactor with and without a NO_x adsorbent at 500 °C

Simple calculation has shown that such electrochemical reactors can be used for purification of real exhaust gas. Really, for a 1.6-l engine for purification of exhaust gas with 500 ppm of NO_x at 400 °C, it requires an electrode area of about 0.9 m^2.

Conclusions

It was shown that the electrochemical reduction of nitric oxide in an atmosphere containing excess oxygen is not effective due to the low selectivity of the cathode materials. To solve the problem of effective electrochemical reduction of nitric oxide in the presence of the excess oxygen Bredikhin et al. [35–37] proposed the concept of artificially designed multilayer structure, which should operate as an electrode with high selectivity. Our investigations have shown that substitution of traditional cathodes by the multilayer electro-catalytic electrode with an electrochemically assembled nanostructure leads to a dramatic decrease in the value of the electrical power required for NO decomposition. It was shown that multilayer electro-catalytic electrode should consist at least three main functional layers: cathode, electro-catalytic electrode, and covering layer, in order to operate as an electrode with high

selectivity. In 2008, Hamamoto et al. [49] proposed to use an electrochemical reactor with fourth additional NO_x adsorption layer. The values of current efficiency in such reactors increase up to 20% and the values of the NO/O_2 selectivity up to 25. These results indicate that this new type of electro-catalytic reactor can be used for practical applications. From our point of view, such systems should substitute traditional catalytic systems for exhaust gas purification.

References

1. Lerdau MT, Munger JW, Jacob DJ (2000) Enhanced: the NO_2 flux conundrum. Science 289(5488):2291–2293
2. Finlayson-Pitts BJ, Pitts JN Jr (1997) Tropospheric air pollution: ozone, airborne toxics, polycyclic aromatic hydrocarbons, and particles. Science 276(5315):1045–1051
3. Libby WF (1971) Promising catalyst for auto exhaust. Science 171:499–500
4. Nishihata Y, Mizuki J, Akao T, Tanaka H, Uenishi M, Kimura M, Okamoto T, Hamada N (2002) Self-regeneration of a Pd-perovskite catalyst for automotive emissions control. Nature 418:164–167
5. Parvulescu VI, Grange P, Delmon B (1998) Catalytic removal of NO. Catal Today 46:233–316
6. Garin F (2001) Mechanism of NOx decomposition. Appl Catal A Gen 222:183
7. Bosch H, Janssen F (1988) Catal Today 2:369
8. Janssen F, Meijer R (1993) Quality control of $DeNO_x$ catalysts Performance testing, surface analysis and characterization of $DeNO_x$ catalysts. Catal Today 16:157
9. Roth JF, Doerr RC (1961) Ind Eng Chem 53:293
10. Baker RA, Doerr RC (1964) J Air Pollut Control Assoc 14:409
11. Baker RA, Doerr RC (1965) Ind Eng Chem Process Des Dev 4:188
12. Klimisch RL, Barnes GJ (1972) Environ Sci Technol 6:543
13. Armor JN (1995) Catalytic reduction of nitrogen oxides with methane in the presence of excess oxygen: a review. Catal Today 26:147–158
14. Iwamoto M (1990) Proceedings of meeting of catalytic technology for removal of nitrogen monoxide. Tokyo, Japan, p 17
15. Hamada H, Kintaichi Y, Sasaki M, Ito T, Tabata M (1990) Appl Catal 64:L1
16. Kintaichi Y, Hamada H, Tabata M, Sasaki M, Ito T (1990) Catal Lett 6:239
17. Sato S, Hirabayashi H, Yahiro H, Mizuno N, Iwamoto M (1992) Catal Lett 12:193
18. Miura K, Nakagawa H, Kitaura R, Satoh T (2001) Low-temperature conversion of NO to N_2 by use of a novel Ni loaded porous carbone. Chem Eng Sci 56:1623–1629
19. Lindsay R, Theobald A, Gießel T, Schaff O, Bradshaw AM, Booth NA, Woodruff DP (1998) The structure of NO on Ni(111) at low coverage. Surf Sci 405:L566–L572
20. Rickardsson I, Jönsson L, Nyberg C (1998) Influence of surface topology on NO adsorption: NO on Ni(100) and Ni(510). Surf Sci 414:389–395
21. Pancharatnam S, Huggins RA, Mason DM (1975) Catalytic decomposition of nitric oxide on zirconia by electrolytic removal of oxygen. J Electrochem Soc 122(7):869–875
22. Gur TM, Huggins RA (1979) Decomposition of nitric oxide on zirconia in a solid state electrochemical cell. J Electrochem Soc 126(6):1067–1075
23. Hibino T (1994) Electrochemical removal of NO and CH_4 from oxidizing atmosphere. Chem Lett 5:927–930
24. Nakatani J, Ozeki Y, Sakamoto K, Iwayama K (1996) NO decomposition in the presence of excess O_2 using the electrochemical cells with Pd electrodes treated at high temperature and coated with La_1-xSrxCoO$_3$. Chem Lett 4:315–316
25. Walsh KJ, Fedkiw PS (1997) Nitric oxide reduction using platinum electrodes on yttria-stabilized zirconia. Solid State Ion 93:17
26. Marwood M, Vayenas CG (1997) Electrochemical promotion of the catalytic reduction of NO by CO on palladium. J Catal 170:275
27. Hibino T, Inoue I, Sano M (2000) Electrochemical reduction of NO by alternating current electrolysis- using yttria-stabilized zirconia as the solid electrolyte; Part I. Characterizations of alternating current electrolysis of NO. Solid State Ion 130:19–29
28. Hibino T, Inoue I, Sano M (2000) Electrochemical reduction of NO by alternating current electrolysis using yttria-stabilized zirconia as the solid electrolyte; Part II. Modification of Pd electrode by coating with Rh. Solid State Ion 130:31–39
29. Iwayama K, Wang X (1998) Selective decomposition of nitrogen monoxide to nitrogen in the presence of oxygen on RuO_2/Ag (cathode)/yttria-stabilized zirconia/Pd(anode). Appl Catal B Environ 19:137
30. Washman ED, Jayaweera P, Krishnan G, Sanjurjo A (2000) Electrocatalytic reduction of NO_x on $La_{1-x}A_xB_{1-y}B'_yO_3$: evidence of electrically enhanced activity. Solid State Ion 136–137:775–782
31. Matsuda K, Kanai T, Awano M, Maeda K (2001) NO decomposition properties of lanthanum manganite porous electrode. MRS Preceding 658, G9, 36, 1–5
32. Hwang HJ, Towata A, Awano M, Maeda K (2001) Sol-gel route to perovskite-type Sr-substituted $LaCoO_3$ thin films and effects of polyethylene glycol on microstructure evolution. Scr Mater 44:2173
33. Simonsen VLE, Find D, Lilliedal M, Petersen R, Kammer K (2007) Spinels as cathodes for the electrochemical reduction of O2 and NO. Top Catal 45:143–148
34. Kammer K (2005) Electrochemical DeNOx in solid electrolyte cells—an overview. Appl Catal B Environ 58:33–39
35. Bredikhin S, Maeda K, Awano M (2001) NO decomposition by an electrochemical cell with mixed oxide working electrode. Solid State Ion 144:1–9
36. Bredikhin S, Maeda K, Awano M (2001) Peculiarity of NO decomposition by electrochemical cell with mixed oxide working electrode. J Electrochem Soc 148(10):D133–D138
37. Awano M, Bredikhin S, Aronin A, Abrosimova G, Katayama S, Hiramatsu T (2004) NOx decomposition by electrochemical reactor with electrochemically assembled multilayer electrode. Solid State Ion 175:605–608
38. Bredikhin S, Abrosimova G, Aronin A, Hamamoto K, Fujishiro Y, Katayama S, Awano M (2004) Pt-YSZ cathode for electrochemical cells with multilayer functional electrode. J Electrochem Soc 151(12):J95–J99
39. Aronin A, Abrosimova G, Bredikhin S, Matsuda K, Maeda K, Awano M (2005) Structure evolution of a NiO-YSZ electrocatalytic electrode. J Am Ceram Soc 88(5):1180–1185
40. Bredikhin S, Abrosimova G, Aronin A, Awano M (2006) Electrochemical cells with multilayer functional electrodes. Part I. Reduction-oxidation reactions in a NiO-YSZ electro-catalytic electrode. J Ion 12(1):33–39
41. Awano M, Fujishiro Y, Hamamoto K, Katayama S, Bredikhin S (2004) Advances in nano-structured electrochemical reactors for

NOx treatment in the presence of oxygen. Int J Appl Ceram Technol 1(2):277–286
42. Hiramatsu T, Bredikhin S, Katayama S, Shiono O, Hamamoto K, Fujishiro Y, Awano M (2004) High selective deNO x electrochemical cell with self-assembled electro-catalytic electrode. J Electroceram 13(1–3):865–870
43. Hamamoto K, Fujishiro Y, Awano M (2006) Intermediate temperature electrochemical reactor for NO*x* decomposition. J Electrochem Soc 153(11):D167–D170
44. Hamamoto K, Fujishiro Y, Awano M (2007) Reduction and reoxidation reaction of catalytic layers in electrochemical cells for NOx decomposition. J Electrochem Soc 154(9):F172–F175
45. Wagner C (1966) In: Delahay P, Tobias CW (eds) Advances in electrochemistry and electrochemical engineering. Interscience Publishers, New York
46. Kobayashi K, Yamaguchi S, Higuchi T, Shin S, Iguchi Y (2000) Solid State Ion 135:643
47. Schoonman J (1988) In: Chowdari BVR, Radakrishna S (eds) Proceedings of the 3rd International Symposium on Solid State Ionics Devices, World Scientific Singapore, 697
48. Bredikhin S, Maeda K, Awano M (2001) Electrochemical cell with two layer cathode for NO decomposition. Ionics 7:109–115
49. Hamamoto K, Fujishiro Y, Awano M (2008) Low temperature NOx Decomposition using electrochemical reactor. J Electrochem Soc 155(8):E109–E111

journal

J. Am. Ceram. Soc., 88 [5] 1180–1185 (2005)
DOI: 10.1111/j.1551-2916.2005.00168.x

Structure Evolution of an NiO–YSZ Electrocatalytic Electrode

Alexander Aronin*, Galina Abrosimova*, Sergei Bredikhin*,†, Kazuyuki Matsuda, and Kunihiro Maeda

Synergy Materials Research Center, AIST, Nagoya 463-8687, Japan

Institute of Solid State Physics, Russian Academy of Science, 142432 Chernogolovka, Russia

Masanobu Awano

Synergy Ceramics Laboratory, FCRA, Nagoya 463-8687, Japan

The microstructure and structural evolution in the composite NiO–YSZ electrocatalytic electrode during operation of electrochemical cells for NO decomposition has been observed and investigated. The structure of the electrocatalytic electrode was found to contain two types of pores. The first group includes pores with a size range of 10–100 nm forming chains or bands. They may form channels by overlapping. These pores are located in YSZ grains and they remain unchanged during cell operation. The second group includes smaller pores located in NiO grains at near-boundary regions with YSZ grains or directly in the NiO–YSZ interface. These regions are unstable during the cell operation and new Ni and NiO grains nucleate and grow in the interfacial areas. The formation of such new grains as a result of the electrochemical processes in the cell has been discussed. The correlation between structure and properties has been studied.

I. Introduction

Recently many efforts have been directed toward exhaust gas purification, with special attention being paid to the development of new effective methods for decomposition of NO gas in lean burn and diesel engines. An electrochemical cell is one such method for the purification of exhaust gas.[1–5] Materials used in electrochemical cells for NO decomposition must comply with many requirements regarding physical and chemical stability. In our previous works,[6–8] we proposed a new family of electrochemical cells for NO decomposition in the presence of excess oxygen. This new type of electrochemical cell can be represented by the following cell arrangement:

(electro-catalytic electrode)|(Pt(cathode))|YSZ|Pt(anode)

In such a cell, the external voltage is applied between the cathode and the anode, and the electrocatalytic electrode covering the cathode is free from voltage drop. The composite oxide electro-catalytic electrode blocks direct penetration of gas molecules to the surface of the YSZ disk and the NO and O_2 gas adsorption takes place at three phase boundaries (tpb) at the surface of the pores inside the electrocatalytic electrode. An external electric field applied between the cathode and anode leads to the polarization of the YSZ solid electrolyte and to the generation of a high concentration of oxygen vacancies in the vicinity of the heterojunction between the cathode and YSZ solid electrolyte. Due to the gradient in the concentration of the oxygen ions between the near cathode region of the YSZ disc and the electrocatalytic electrode, the diffusion of oxygen ions from the electrocatalytic electrode to YSZ takes place. Diffusion of mobile oxygen ions from the electrocatalytic electrode to the YSZ solid electrolyte leads to the generation of a high concentration of oxygen vacancies inside the electrocatalytic electrode and, as a result, to adsorption and decomposition of NO and O_2 gas molecules at tpb at the surface of the pores inside the electrocatalytic electrode. It was recently shown that the best properties were obtained for the samples containing nanopores in the as-prepared structure.[7,8] During a high-temperature operation, the generation of a high concentration of oxygen vacancies inside the electrocatalytic electrode, and oxygen ionic transport from the electrocatalytic electrode to the anode can drastically change the microstructure and the catalytic properties of the electrochemical cell. At the same time, the changes in the microstructure may lead to the degradation of the cell during the cell operation.

In this study, we have examined in detail the microstructure and phase transformation during the operation of an NiO YSZ electrocatalytic electrode covering a Pt cathode.

II. Experimental Procedure

The arrangement of the electrochemical cell is schematically illustrated in Fig. 1. The electrochemical cells were constructed from YSZ disc (Mino Ceramic), Pt paste (TR-707, Tanaka Kikinzoku Kogyo), and NiO–YSZ composite oxide paste, which were produced by the following method. NiO powder (Soekawa Chemical) and YSZ powder (8 mol% yttria-stabilized zirconia, TZ-8Y, Tosoh) were used for the preparation of an NiO–YSZ mixed oxide. The NiO–YSZ pastes were prepared by mixing the obtained mixtures and polyethylene glycol ($HOCH_2(CH_2OCH_2)_nCH_2OH$, MW = 300).

A YSZ disc with a thickness of 500 μm and a diameter of 20 mm was used as the solid electrolyte. The Pt paste was screen-printed with an area of 1.77 cm^2 on one surface of the YSZ disk as the cathode, and then calcined at 1473 K for 20 min. The NiO–YSZ paste was screen-printed with an area of 2 cm^2 over the cathode and sintered. The printed layer of NiO–YSZ mixed oxide paste was sintered at 1773 K for 4 h. The Pt paste was screen-printed with an area of 1.77 cm^2 on the other surface of the YSZ disk as the anode, and then calcined at 1473 K for 20 min. Platinum mesh and wire were attached to the cathode and the anode, for connection with the power supply unit.

The structure of the cells was studied by scanning, transmission, and high-resolution electron microscopy and X-ray diffraction. X-ray diffraction experiments were performed using a Rigaku RINT2000 diffractometer with Cu$K\alpha$-radiation. Special computer programs were used for the separation of overlapped

E. D. Wachsman—contributing editor

Manuscript No. 187049. Received April 8, 2002; approved July 14, 2004.
Work supported by METI, Japan, as part of the Synergy Ceramics Project. Part of the work supported by NEDO and by a grant of the Russian Academy of Science "New Materials and Structures."
*Institute of Solid State Physics, Russian Academy of Science, Chernogolovka, Russia.
†Author to whom correspondence should be addressed. e-mail: bredikh@issp.ac.ru

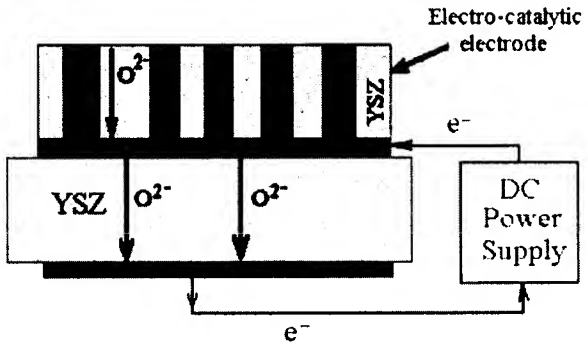

Fig. 1. Conceptual representation of the electrochemical cell with a composite electrocatalytic electrode for NO_x decomposition.

reflections in the X-ray diffraction patterns and for the determination of the peak halfwidth. Diffraction experiments with an Al standard were carried out for the determination of the lattice parameter change. The transmission and high-resolution electron microscopy investigations were carried out on JEOL 4000 FX and JEOL 2010 F microscopes (JEOL, Tokyo, Japan). Foils for the electron microscopy investigations were prepared by mechanical polishing followed by ion milling. A scanning electron microscope JSM-6330F/JED-2140 was used to study the microstructure and chemical element distribution through the cross-section of the YSZ NiO electrode.

III. Experimental Results and Discussion

Measurements of the nitrogen monoxide decomposition for electrochemical cells with mixed oxide NiO (45 vol%)–YSZ(55 vol%) electrocatalytic electrode sintered at 1773 K for 4 h showed that the experimentally measured dependencies of NO conversion rate on the value of the current were linear (Fig. 2) and follow the calculated one at 1000 ppm of NO and 3% of O_2 in He(balance) at a flow rate v = 50 mL/min.[7,8] In our previous works,[6–8] we have shown that for an electrochemical cell with nano-porous electrocatalytic electrode, the probability for NO and O_2 gas adsorption and decomposition is the same, and as a result, the dependence of NO conversion rate on the value of the current should be linear and the value of the current efficiency should depend only on the NO and O_2 gas concentration in accordance with a Faradaic reaction ($\eta_{calc} = [NO]/([NO]+2[O_2])$). In Fig. 2, the NO conversion is plotted as a function of the current of the as-manufactured cell (curve 1) and after cell operation for 5 and 12 h (curves 2 and 3 respectively). Figure 3 shows the current–voltage characteristics of the as-manufactured cell and after cell operation at 600°C for 5 and 12 h. It is seen that the characteristics of the cell are stable and reproducible at a cell operating voltage lower than 2.2 V.

To investigate the processes occurring during the operation of the electrochemical cell, investigations of the electrocatalytic electrode microstructure have been carried out before and after cell operation.

(1) The Structure of the Electrocatalytic Electrode Before Operation

The structure of the electrocatalytic electrode sintered at 1773 K consists of YSZ and NiO grains. The average grain size of both NiO and YSZ was about 1 μm. The surface of the electrocatalytic electrode before operation is shown in Fig. 4. No peculiarities of grain size and of the grain morphology were observed.

However, careful investigations reveal some specific features of the structure. In particular, pores of different sizes have been observed. The pores may be divided into two groups according to their size and location.

The first group of pores has spherical or ellipsoidal shape and it presents chains and bands of pores. The pores often cross several grains (as a rule, YSZ grains). In a number of cases, the pores overlap forming channels (Figs. 5 and 6). Figure 5 shows the typical microstructure of a sample sintered at 1773 K. It contains a pore chain crossing some grains. The pore size is 10–100 nm and some of the pores are overlapped. Pore bands are shown in Fig. 6. Some of them overlap, forming the channels. The diameter of these channels is 30–40 nm.

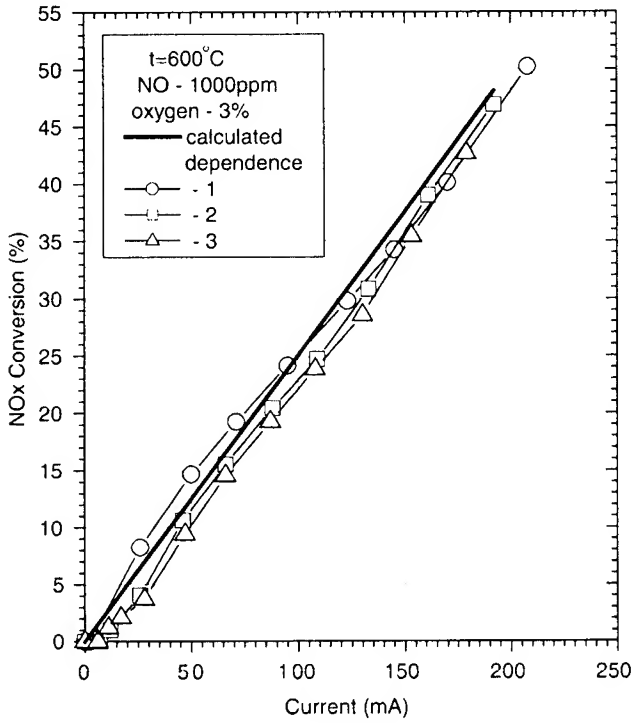

Fig. 2. The dependence of NO conversion on the value of the current for the as-manufactured cell (curve 1) and after cell operation for 5 and 12 h (curves 2 and 3). Reactant gas: 1000 ppm of NO and 3% of O_2 in He at gas flow rate 50 mL/min.

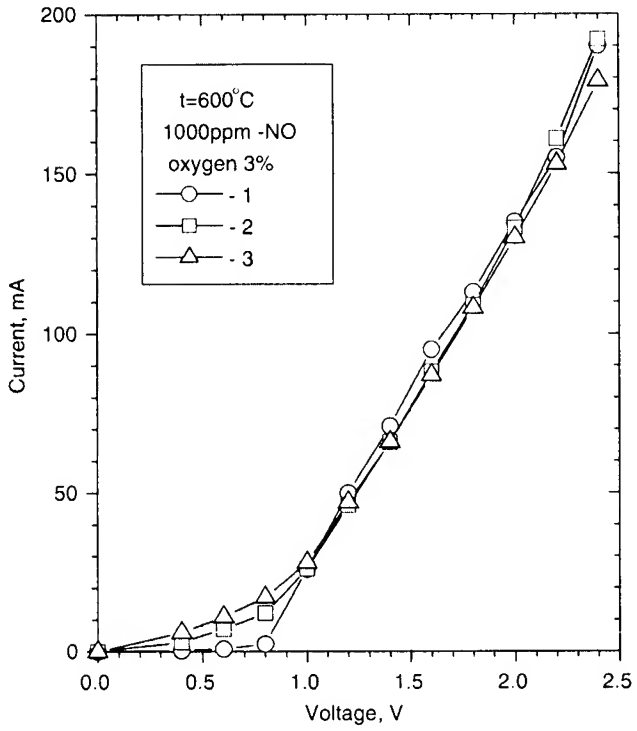

Fig. 3. Current–voltage characteristics for the as-manufactured cell (curve 1) and after cell operation for 5 and 12 h (curves 2 and 3).

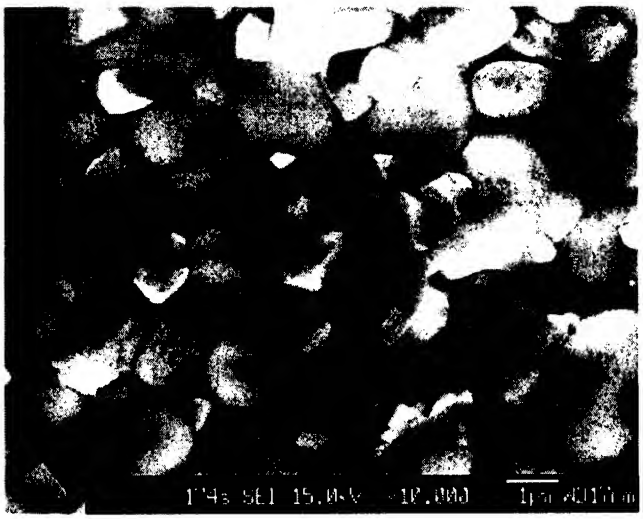

Fig. 4. SEM image of the electrocatalytic electrode surface.

The second group of pores is associated with interfacial boundaries between NiO and YSZ grains. These interfacial boundaries were found to have structural peculiarities. As-prepared samples contain regions with pores located near and in the interfacial boundaries. The thickness of the regions is about 30–40 nm. The pores sized 5–30 nm have either spherical or ellipsoidal shape, or they form channels of the same diameter with a length of some hundreds of nanometers. Figure 7 shows the boundary between YSZ and NiO grains, which is sloping to electron beam, and the pores and the channels are clearly visible. These channels and pores may overlap, forming a thin, three-dimensional near-boundary zone. Special electron microscopy investigations have been carried out in order to determine on which side of the boundary this pore zone is located. The results are given in Fig. 8. This figure shows an interfacial boundary containing the pore zone. Diffraction patterns from bordering grains are inserted. The YSZ grain is determined to be to the right and the NiO grain is to the left. The location of the grain was also confirmed by EDS method. Figures 8(b) and (c) show the dark field electron microscopy images of the grains in the reflections marked by arrows in the diffraction patterns (Fig. 8(a), insets). It means that Fig. 8(b) shows only the NiO grain and Fig. 8(c) shows the YSZ grain. The pore zone noted in Fig. 8(a) is only in the NiO grain; it is marked by arrows. This situation is typical for the structure. Therefore, the pore zone is located in the near-boundary region of NiO grains. No peculiarities were observed in the near-boundary YSZ–YSZ regions and in the near-boundary NiO–NiO regions. The presence of the observed pore regions makes the boundaries more permeable for the gas and increases the reaction zone for NO decomposition.

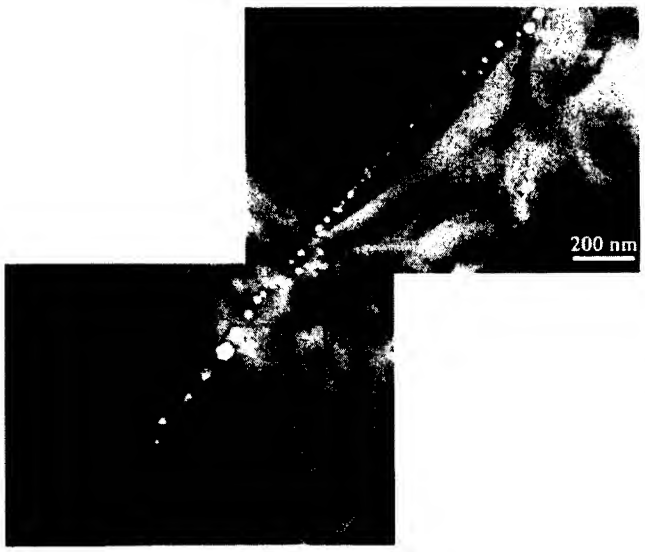

Fig. 5. TEM image of the microstructure of the as-prepared sample.

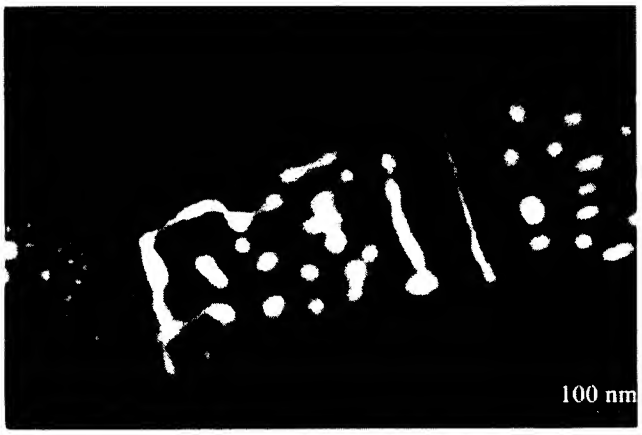

Fig. 6. TEM image of overlapped pores in the as-prepared sample.

The structure of the electrocatalytic electrode was also studied by X-ray diffraction. The X-ray diffraction patterns contain reflections from YSZ, NiO, and Pt. No signs of any additional phase were observed.

(2) The Structure of the Electrocatalytic Electrode After Operation

The X-ray diffraction patterns of the electrocatalytic electrode of the as-prepared cell and following operation for 22 h at 600°C at cell-operating voltage lower than 2 V and at average value of the current through the cell order of 90 mA are represented in Fig. 9. In addition to the phases mentioned above, very weak reflections corresponding to Ni crystals have been observed in the X-ray diffraction pattern after the cell operation. These reflections are marked by triangles in the figure, and show that the structure of the electrocatalytic electrode also contains Ni grains after the cell operation. The intensity of Ni reflections was very weak and the amount of Ni grains is small.

The NiO reflections are located at the same positions in both the as-prepared sample and in the sample after operation. The half-width of the diffraction lines increases in the cell after operation and $K\alpha_1 K\alpha_2$ splitting decreases. These changes of the diffraction lines indicate a decrease of the average grain size of NiO particles. This indicates the appearance of new NiO grains during the cell operation. Similar modifications (although weaker) of YSZ reflections have also been observed, showing that the

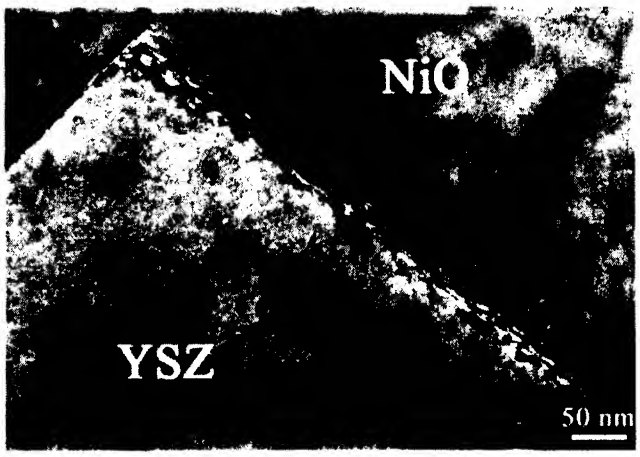

Fig. 7. TEM image of an interfacial boundary between YSZ and NiO grains.

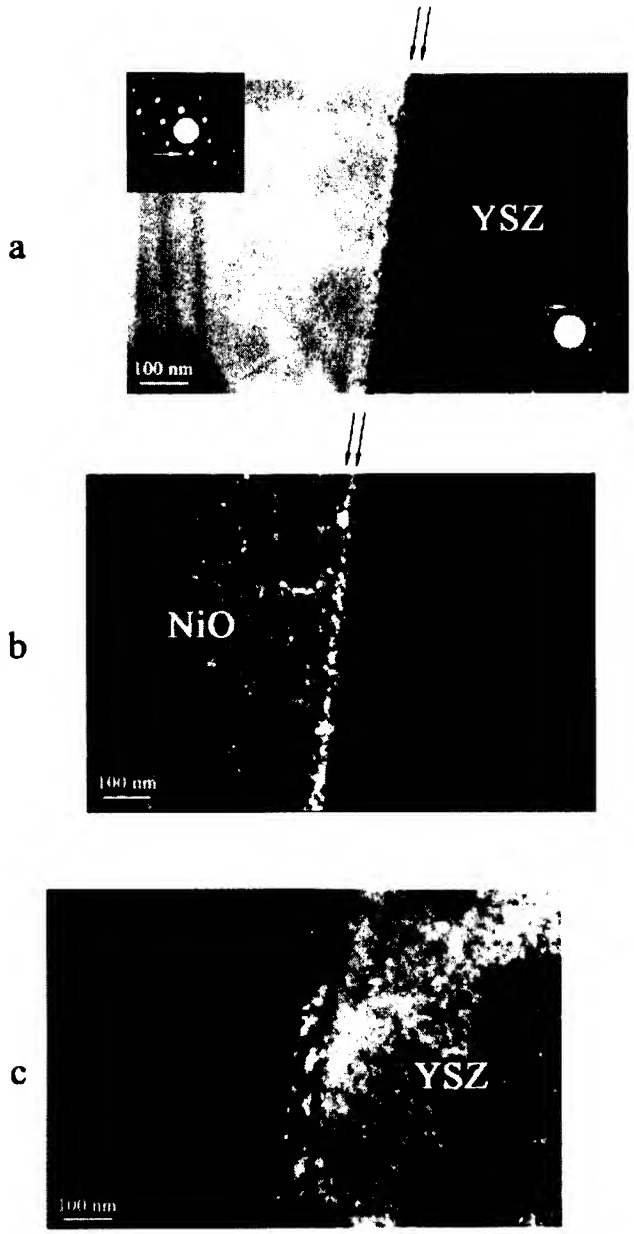

Fig. 8. Bright field TEM image (a) and dark field TEM images (b, c) of the interfacial boundary containing the pore zone.

average grain size of YSZ particles also decreases. In addition, the YSZ reflections were slightly shifted to larger diffraction angles, i.e., the YSZ lattice parameter slightly decreases. This decrease of YSZ lattice parameter may be caused by the formation of a high concentration of oxygen vacancies during the cell operation.

The microstructure of the electrocatalytic electrode also changes. The essential changes occur in the interfacial boundary region between NiO and YSZ grains. After the electrochemical cell operation for 22 h at a cell voltage lower than 2.2 V, they are as follows:

(1) New grains nucleate and grow in the pore zone of NiO near-boundary regions. The zone of new grains spreads into the depth of the NiO grain (Fig. 10). In some cases, this zone of new grains devours "old" NiO grain completely (Figs. 11(a) and (b)). The electron diffraction patterns from these regions contain ring reflections of Ni in addition to NiO reflections. The size of Ni grains is 5–20 nm and they are seen in the dark field electron microscopy image (Fig. 11(b)). This image was obtained in the reflection marked by the arrow in the electron diffraction pattern (Fig. 11(a), inset). The new grains are both Ni and NiO phases.

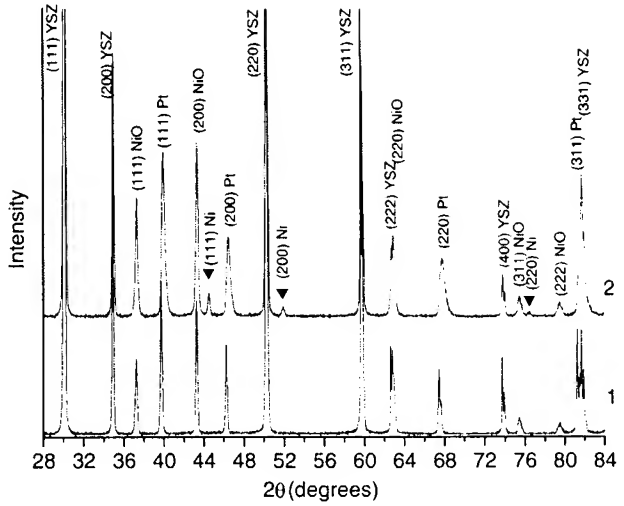

Fig. 9. X-diffraction patterns of the as-prepared sample (1) and the sample after operation (2).

(2) In the region with new NiO grains, the pores are located both in the interfacial vicinity and before the front of new growing grains. Sometimes, small NiO grains are surrounded by the pores on all sides. Separate pores are also observed in the region of new grains, located between the new grains (Fig. 10). The high-resolution electron microscopy images of the near-boundary region of YSZ grain and small NiO grain formed during the cell operation at different magnifications are shown in Fig. 12. The size of the new NiO grains varies from 10 to 100 nm depending on the location.

(3) An orientation relationship has been found to exist between the lattices of YSZ and new NiO grains:

$$(310)_{YSZ}||(110)_{NiO},[001]_{YSZ}||[1\bar{1}1]_{NiO}$$

The presence of the orientation relationship between the lattices of YSZ and NiO grains indicates that the new NiO grains may nucleate on the YSZ grains as on the substrate, and in this case, their surface energy will decrease.

The lattice parameter of the YSZ grains determined from the HREM images is less in the near-boundary region than in the depth of the grain. According to the X-ray diffraction data, the lattice parameter of YSZ slightly decreases as well.

Pore chains crossing the YSZ grains (the first group of pores) have been also observed in the structure after cell operation. A view of these pores is similar to the view of the pores observed in as-prepared samples. Nucleation of new grains on the pores and near the pores inside YSZ grains was not found. Figure 13

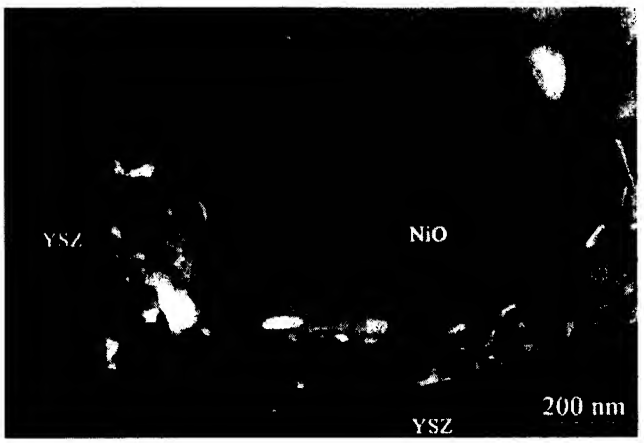

Fig. 10. Interfacial boundary between YSZ and NiO grains of the sample after cell operation.

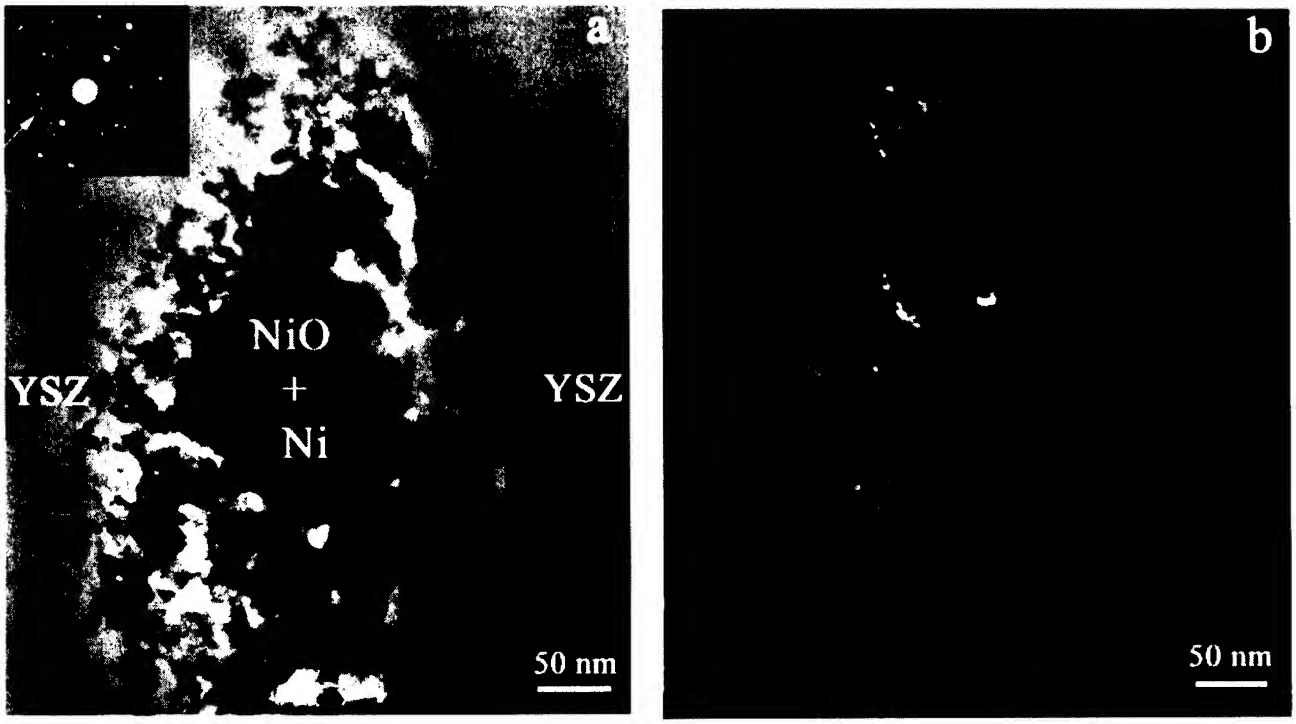

Fig. 11. Bright field TEM image (a) and dark field TEM images (b) of new NiO and Ni grains zone that devoured "old" NiO grain.

shows the channels from the pores located in the direct vicinity of the interfacial boundary. These chains disappear completely if they cross NiO grains at the site of new grain formation.

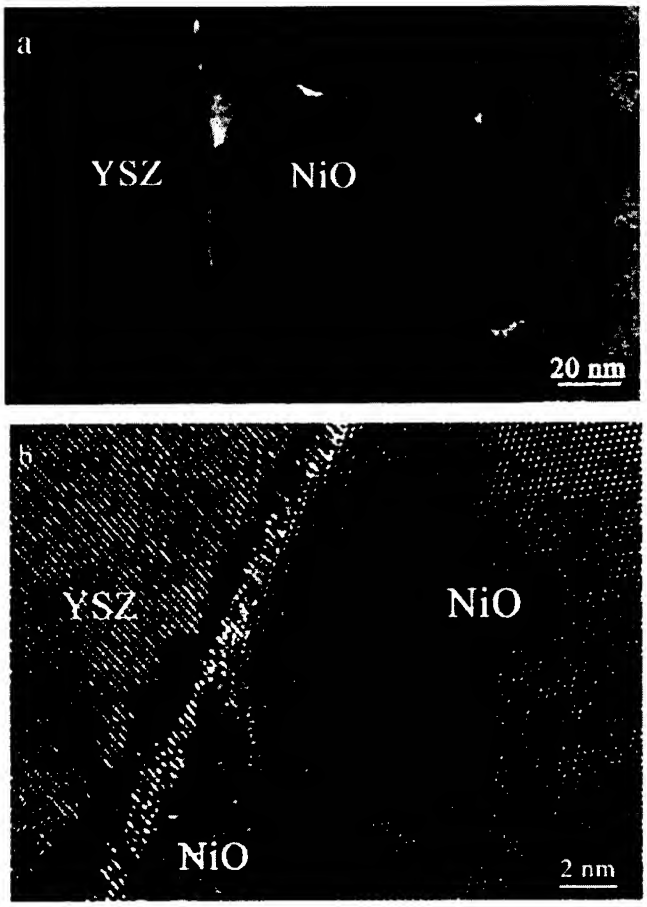

Fig. 12. HREM images of a near-boundary region of a YSZ grain and small NiO grains formed during the cell operation (magnifications in a and b different).

A cross-sectional view of the electrocatalytic electrode after the electrochemical cell operation for 22 h is shown in Fig. 14. It is seen that NiO and YSZ particles produce a three-dimensional network of pathways for electron and oxygen ion migration, respectively. No change was observed at the interfaces between the grains inside the NiO and YSZ networks, and the boundaries between the NiO/NiO and YSZ/YSZ grains remain smooth during the cell operation. At the same time, a drastic change of the microstructure takes place at the interface between YSZ and NiO networks. It is observed that the interfaces between NiO and YSZ grains exhibit morphological changes and the formation of a large amount of small grains with a typical size smaller than 100 nm on the NiO/YSZ interface takes place.

In order to understand the structure evolution during the cell operation, one should consider the mechanism of NO and O_2 gas adsorption and decomposition. As was mentioned previously, an external voltage applied between the cathode and anode leads to the polarization of the YSZ solid electrolyte and to the generation of a high concentration of oxygen vacancies in

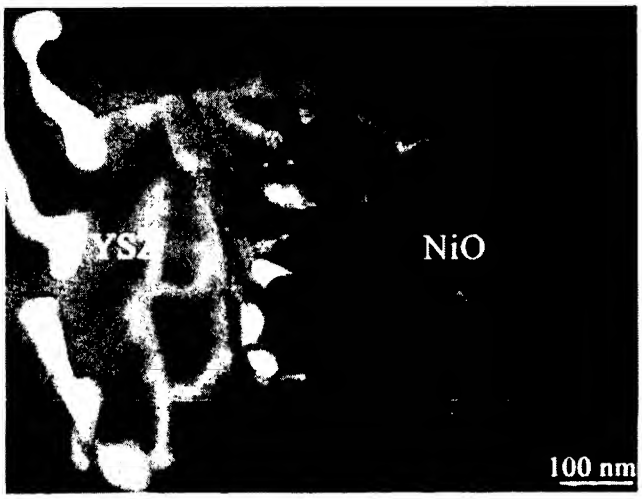

Fig. 13. TEM image of pore channels from the pores in the direct vicinity of the interfacial boundary.

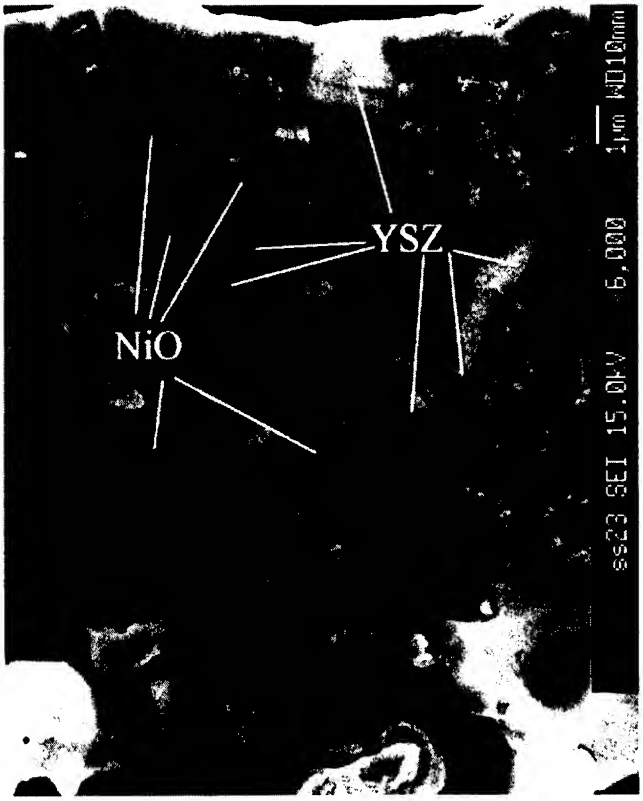

Fig. 14. SEM image of the cross-section of the electrocatalytic electrode after cell operation.

the near cathode region of the YSZ solid electrolyte and in the three-dimensional network of YSZ particles inside the electrocatalytic electrode. It is well known that in the temperature region of 600°–900°C, NiO can be easily reduced to Ni under reducing conditions, and vice versa: Ni can be easily oxidized to NiO in the presence of excess oxygen. The formation of new Ni and NiO grains in the YSZ/NiO boundary and in the near-boundary layers means that the process of NiO reduction begins at these locations. Under the applied voltage, NiO transforms to Ni and oxygen is removed through the electrode. At the same time, Ni oxidation and the appearance of new NiO grains occurs due to the penetration of oxygen and NO gases through the pores between NiO and YSZ grains. This second group of pores plays an important role in the oxidation–reduction reaction. They provide three-dimensional zones (nets) of lower density, simplifying the access of the gases and increasing the reaction surface. Therefore, the reduction of NiO grains into Ni grains and the oxidation of Ni grains into NiO takes place continuously during cell operation.

IV. Conclusions

The structure of the NiO–YSZ electrocatalytic electrode of an electrochemical cell was found to contain pores of two types. The first type includes the pores with a size of 10–100 nm. These pores may form chains or lengthy zones and they may form channels by overlapping. The second type includes pores situated in the near-boundary regions of the YSZ–NiO interface. They are located on the NiO side of the boundary and provide an enhanced gas permeability of such boundaries. In these regions, new Ni and NiO grains nucleate and grow during the cell operation at 873 K.

The structure evolution in the vicinity of YSZ/NiO interfaces permits the conclusion that the processes of NO and O_2 gas adsorption and decomposition take place on the interface between NiO and YSZ grains, and that the formation of a high concentration of small size NiO grains is a result of such processes. The Ni grains appearing during the cell operation may play an important role both in the structure evolution and in the electrocatalytic properties of the cell.

Acknowledgments

The authors are members of the Joint Research Consortium of Synergy Ceramics.

References

[1]S. Pancharatnam, R. A. Huggins, and D. M. Mason, "Catalytic Decomposition of Nitric Oxide on Zirconia by Electrolytic Removal of Oxygen," *J. Electrochem. Soc.*, **122** [7] 869–75 (1975).

[2]T. M. Gur and R. A. Huggins, "Decomposition of Nitric Oxide on Zirconia in a Solid State Electrochemical Cell," *J. Electrochem. Soc.*, **126** [6] 1067–75 (1979).

[3]T. Hibino, "Electrochemical Removal of NO and CH_4 from Oxidizing Atmosphere," *Chem. Lett.*, **23** [5] 927–31 (1994).

[4]J. Nakatani, Y. Ozeki, K. Sakamoto, and K. Iwayama, "NO Decomposition in the Presence of Excess O_2 Using the Electrochemical Cells with Pd Electrodes Treated at High Temperature and Coated with $La_{1-x}Sr_xCoO_3$," *Chem. Lett.*, **25** [4] 315–9 (1996).

[5]E. D. Washman, P. Jayaweera, G. Krishnan, and A. Sanjurjo, "Electrocatalytic Reduction of NO_x on $La_{1-x}A_xB_{1-y}B'_yO_3$: Evidence of Electrically Enhanced Activity," *Solid State Ionics*, **136–137**, 775–82 (2000).

[6]S. Bredikhin, K. Maeda, and M. Awano, "Electrochemical Cell with Two Layers Cathode for NO Decomposition," *J. Ionics*, **7**, 109–15 (2001).

[7]S. Bredikhin, K. Maeda, and M. Awano, "NO Decomposition by an Electrochemical Cell with Mixed Oxide Working Electrode," *Solid State Ionics*, **144**, 1–9 (2001).

[8]S. Bredikhin, K. Maeda, and M. Awano, "Peculiarity of NO Decomposition by Electrochemical Cell with Mixed Oxide Working Electrode," *J. Electrochem. Soc.*, **148** [10] D133–8 (2001).

Journal of the Ceramic Society of Japan, Supplement 112-1, PacRim5 Special Issue, 112 [5] S1071-S1074 (2004)

Paper

Microstructure-Controlled High Selective DeNO$_x$ Electrochemical Reactor

Koichi HAMAMOTO, Takuya HIRAMATSU,* Osamu SHIONO,* Shingo KATAYAMA,* Yoshinobu FUJISHIRO, Sergei BREDIKHIN** and Masanobu AWANO

Synergy Materials Research Center, AIST, Shimo-Shidami, Moriyama-ku, Nagoya 463-8687, Japan
**Synergy Ceramics Laboratory, FCRA, Shimo-Shidami, Moriyama-ku, Nagoya 463-8687, Japan*
***Institute of Solid State Physic Russian Academy of Science, 142432 Chernogolovka, Russia*

We proposed and investigated a new type of solid-state electrochemical reactor for NO$_x$ decomposition. The electrolyte by covering of composite Pt-YSZ cathode with a NiO-YSZ electro-catalytic electrode for enhancing the selective decomposition of NO$_x$ gas was designed. The structure of the electro-catalytic electrode was found to contain self-assembled nano-pores and ionic-electronic conducting network. The nano-pores were located in NiO grains, either near boundary regions of YSZ grains or at the NiO-YSZ interface. These regions have two kinds of active sites provides a way to suppress the unwanted reaction of oxygen gas adsorption and to increase many times the desirable reaction of NO gas decomposition. The correlation between the structure and properties was also studied and reported. [Received August 8, 2003; Accepted December 24, 2003]

Key-words : *NO decomposition, Electrochemical reactor, Self-assemble, Nano-pore ceramic, NiO-YSZ*

1. Introduction

Nitrogen oxides, NO and NO_2 are emitted together with H_xC_y and CO from diesel and lean-burning engines. Ozone (O_3), which is the principal toxic component of smog in large cities and a greenhouse gas, is produced through a photolytic decomposition of nitrogen oxide radicals (NO_x) by solar irradiation. NO_x is also harmful to the environment as it contributes to the acid rain.[1),2)] Therefore, there has been a great demand for an effective method of the purification of the exhaust gas. There is no effective method for NO_x decomposition, especially in the presence of excess oxygen. Without coexisting oxygen the successful decomposition of NO gas into oxygen and nitrogen in a primitive electrochemical cell was first demonstrated by Huggins et al.[3),4)] They showed that by applying an electric field or current to a YSZ-based cell, NO can be decomposed into nitrogen gas and oxygen ion at the cathode, and the oxygen ion can be pumped through the solid electrolyte to the anode. Unfortunately, in the presence of oxygen a high current density is required for NO reduction because the coexisting oxygen is adsorbed and decomposed by the cathode in preference to the NO gas. Recently, many attempts have been carried out to improve the properties of electrochemical cells by using different catalysts as cathode materials.[5)-9)]

In our previous works we proposed a new family of electrochemical cell for NO decomposition in the presence of excess oxygen.[8)-10)] This type of electrochemical cell can be represented by the following cell arrangement:

(Electro-catalytic electrode) | (Cathode) | YSZ | (Anode) (1)

The electro-catalytic electrode blocks the direct penetration of gas molecules to the surface of YSZ disk and the NO and O_2 gas adsorption takes place at the surface of pores inside the electro-catalytic electrode. In our previous works a strong correlation between the process of NO decomposition and the microstructure and composition of the electro-catalytic electrode was observed.[8)-10)] It showed that the increase of ambipolar conductivity of the electro-catalytic electrode resulted in a decrease of the cell operating voltage and in a decrease in the electrical power required for NO decomposition.[11),12)] However, the increase in electronic conductivity of electro-catalytic electrode of this electrochemical cell not only improves the efficiency, but also increases the oxygen adsorption and decomposition on the surface of electro-catalytic electrode. In fact, the formation of three-dimensional networks of Ni grain layers connected with the cathode leads to effective electronic transport to the surface of electro-catalytic electrode followed by an effective oxygen gas adsorption on the open surface of YSZ grains.

In the present study, we proposed to deposit an additional insulating upper layer on the surface of self-assembled electro-catalytic electrode, to prevent oxygen gas adsorption on the open surface of the electro-catalytic electrode. Also, we investigated the electro-catalytic properties of new type of electrochemical reactor with multi-layer electrode for NO decomposition and correlated with the changes of microstructure in the electro-catalytic electrode during the cell operation.

2. Experimental

The new type of electrochemical reactor with multi-layer electrode for decomposition of NO gas in the presence of excess oxygen can be represented by the following cell arrangement:

YSZ | (Electro-catalytic electrode) | (Cathode) | YSZ | Pt (Anode) (2)

A YSZ disk with a thickness of 0.5 mm and a diameter of 20 mm was used as an oxygen ionic conductor for manufacturing of the electrochemical cell. The Pt-YSZ composite paste was screen-printed with an area of 1.77 cm^2 on the surface of YSZ disc as the cathode and calcined at 1673 K for 1 h. Then the mixed oxide of NiO-YSZ paste with 50 mol% of NiO was screen-printed with an area of 2.01 cm^2 over the cathode and sintered at 1723 K for 3 h. The YSZ paste was screen-printed with an area of 2.01 cm^2 over the electro-catalytic electrode and calcined at 1473 K for 1 h. The Pt paste was screen-printed with an area of 1.77 cm^2 on to the other surface of YSZ disk as the anode and calcined at 1473 K for 20 min. Platinum wire was attached to the cathode and the anode, to connect with the power supply unit.

The electrochemical reactor was set in the quartz reactor and connected to the potentio-galvanostat (SI1287 and 1255B, SOLARTRON), to investigate the applied voltage and current dependence of NO decomposition behavior. The range of applied voltage to the electrochemical cell was between 0 and

3 V. The electrochemical decomposition of NO was carried out at 773 K, 798 K, 823 K and 873 K, respectively by passing a mixed gas with 1000 ppm of NO ($[NO]_{in}$) and 2% of O_2 in He through the cell at a gas flow rate of 50 ml/min. Mass flow controllers were employed to obtain a well-defined gas mixture of NO, O_2 and He. The concentrations of NO and N_2 in the outlet gas ($[NO]_{out}$) were monitored using an on-line NO_x (NO, NO_2 and N_2O) gas analyser (Best Instruments BCL-100uH, BCU-100uH) and a gas chromatograph (CHROMPACK Micro-GC CP 2002), respectively. The conversion of nitrogen monoxide (ΔNO), based on these measurements was calculated as:

$$\Delta NO = ([NO]_{in} - [NO]_{out})/[NO]_{in}. \quad (3)$$

For investigation of NiO-YSZ electro-catalytic electrode, the microstructure of experimental cells was cut off into two parts through the center of the disk. The microstructure and chemical element distribution through the cross-section of NiO-YSZ electrode were examined by using a scanning electron microscope (JSM-6330F/JED-2140).

3. Results and discussion

In **Figs. 1** and **2**, the NO conversion in an electrochemical reactor with multi-layer electrode under various cell-operating temperatures as a function of current and electrical power are plotted, respectively. The calculated dependence of NO conversion rate on the value of current at 1000 ppm of NO and 2% of O_2 in He (balance) at a flow rate $v = 50$ ml/min is shown in Fig. 1. From these figures, it is seen that the efficiency of NO decomposition by new type of electrochemical cell with the functional multi-layer electrode is much better than the efficiency of the traditional type of electrochemical cells[13] at a low operating temperature, especially at 773 K. This result supports our proposal that the deposition of insulating upper layer should suppress the oxygen gas adsorption and decomposition on the open surface of electro-catalytic electrode. As temperature increased, more current and electrical power were required for NO decomposition. These results suggest that a lot of oxygen pumping has occurred at higher operating temperature.

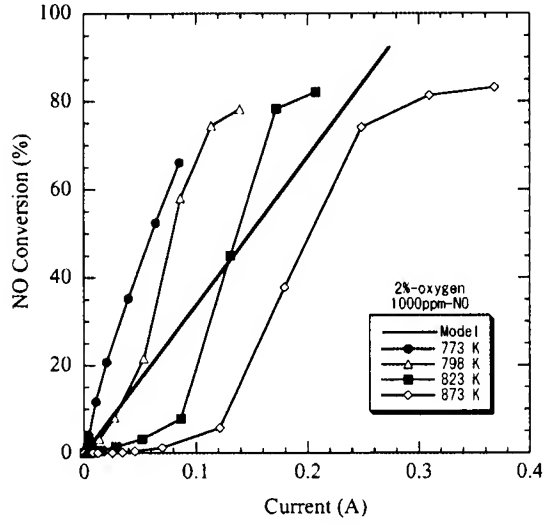

Fig. 1. Dependence of NO conversion on current passing through the electrochemical reactor with multi-layer electro-catalytic electrode at different cell operating temperatures. Reactant gas: 1000 ppm of NO and 2% of O_2 in He (balance) at a gas flow rate of 50 ml/min.

Figure 3 shows the current efficiency (η) of the electrochemical reactor calculated from the data of Fig. 1. We can calculate the theoretical value of current efficiency (η_{calc}) of an electrochemical cell as a ratio between NO gas concentration and the sum of NO gas concentration and double oxygen gas concentration,

$$\text{i.e., } \eta_{calc} = [NO]/([NO] + 2[O_2]). \quad (4)$$

Equation (3) follows that the dependence of NO conversion rate on the value of the current should be linear and the value of current efficiency should depend only on the NO and O_2 gas concentration, if there is no gas selectivity. The electrochemical cell shows high current efficiency over 3 times of the theoretical value ($\eta_{calc} = 2.44\%$) at 773 K. In our previous works,[9),13)] we obtained the measured values of current efficiency of the electrochemical cell without insulating upper layer was equal to the calculated value. These results confirm

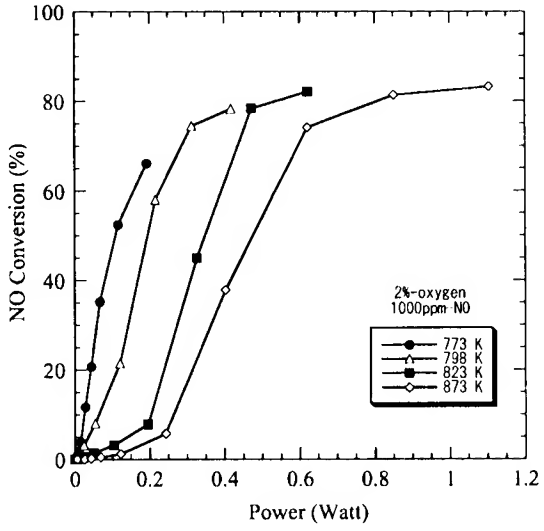

Fig. 2. Dependence of NO conversion on electric power consumption applied to the electrochemical reactor with multi-layer electro-catalytic electrode at different cell operating temperatures.

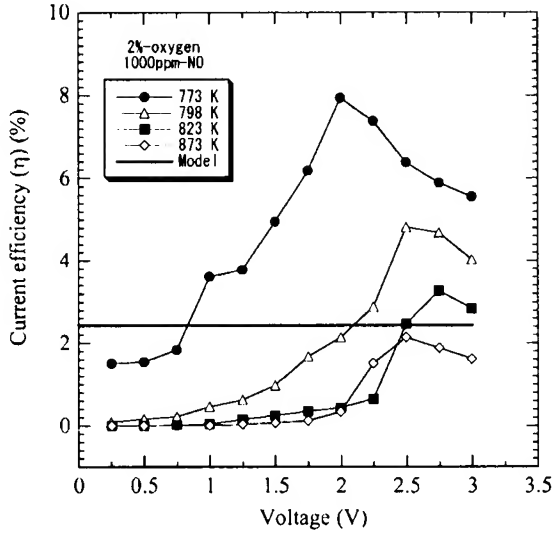

Fig. 3. Dependence of current efficiency for decomposition of NO on operating voltage at different cell operating temperatures.

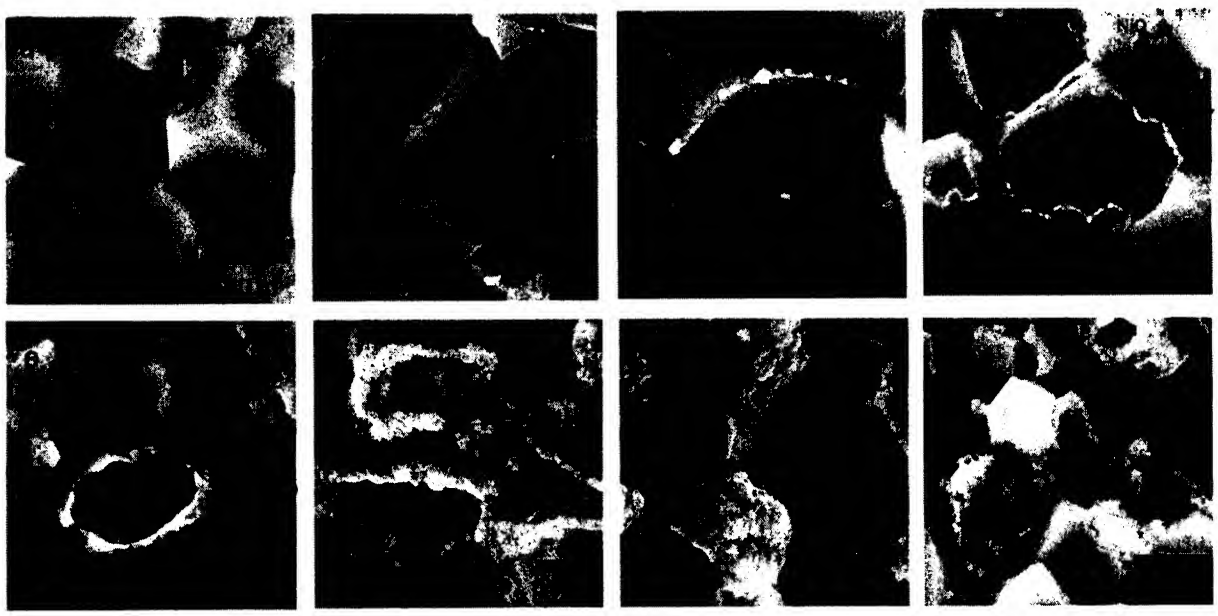

Fig. 4. The SEM micrograph of the cross-section view of the electro-catalytic electrode. (a) as-sintered and (b) to (h) after cell operation at 798 K under applied voltages of 1.00, 1.50, 2.00, 2.25, 2.50, 2.75 and 3.00 V for 15 min, respectively.

that, it is possible to increase the selectivity of NO decomposition by the existence of YSZ upper layer. It is also seen that the value of current efficiency is decreased at higher cell operating voltage and temperature.

The above mentioned result can be explained by the correlation with structural changes of electro-catalytic electrode. **Figure 4** shows the SEM micrograph of the cross-section view of the electro-catalytic electrodes. Figure 4(a) shows the microstructure of as-sintered electro-catalytic electrode (b) to (h) shows the microstructure of the electro-catalytic electrode after cell operation at 798 K under applied voltages of 1.00, 1.50, 2.00, 2.25, 2.50, 2.75 and 3.00 V for 15 min, respectively. From the Fig. 4, it is seen that new grains are nucleated and grown in the YSZ/NiO and NiO/NiO interface boundary regions. The zone of new grains spreads into the depth of NiO grain under the applied voltage. As the applied voltage is increased, the more Ni grains are nucleated and grown on the surface to inside the NiO grains. The cores of NiO grains of less than 1 μm size are reduced to Ni grains under the applied voltage of 3 V. As a result, a lot of pores on the surface of YSZ grains with F-type centers in the electro-catalytic electrode were formed at the same time.

It is well known that the adsorption and decomposition of NO gas molecules occurs on the surface of Ni grains preferably, in the presence of oxygen gas molecules.[14),15)] The following reaction mechanism is proposed for NO decomposition on the nano-size Ni grains formed near interface boundary porous region between the grains of NiO and YSZ during the cell operation.

$$NO + Ni \rightarrow Ni - NO. \quad (5)$$

$$2Ni - NO \rightarrow 2NiO + N_2. \quad (6)$$

NO gas molecules are first chemisorbed on Ni and then decompose to form N_2 and NiO. The oxygen ionic current passed through the network of YSZ particles surrounding the Ni grains removed the oxygen species and permitted the reaction to reoccur. The regeneration reaction of the reduction of NiO to Ni takes place permanently at the NiO/YSZ interface under the cell operation

$$NiO + V_O(ZrO_2) + 2e^- \rightarrow Ni + O^{2-}(ZrO_2). \quad (7)$$

As a result the catalytic activity for NO decomposition is independent of the operation time. At the same time oxygen gas molecules have a preference for adsorption by F-type centers on the surface of YSZ

$$O_2 + 4e^- + V_O(ZrO_2) \rightarrow 2O^{2-}(ZrO_2). \quad (8)$$

From this consideration it follows that under the cell operation adsorption and decomposition of NO and O_2 gas molecules occur on the surface of Ni grains and by F-type centers on the surface of YSZ grains, respectively.

When low voltage is applied to the cell, the upper layer leads to suppressing of the oxygen gas adsorption and to an appropriate amount of concentration of the oxygen vacancies in the YSZ grains. As a result it increases the rate of reduction of NiO to Ni and the amount of new Ni grains in the YSZ/NiO and NiO/NiO thin interface region. Therefore the electrochemical cells with multi-layer electrode should show a much higher selectivity for NO_x gas decomposition.

However high voltage is applied to the cell, a lot of pores and open surface of YSZ grains were formed by the excessive reaction of the reduction of NiO to Ni. As a result, the efficiency of NO decomposition is decreased. Therefore the electrochemical reactor with multi-layer electrode should operate much lower operating voltage and temperature for an effective NO decomposition in the presence of excess oxygen.

4. Conclusions

The electrochemical reactor with multi-layer electrode shows an effective NO decomposition in the presence of excess oxygen at 773 K. The electrochemical reactor shows high current efficiency over 3 times of the theoretical value at 773 K. Catalytic properties are investigated and correlated with the structural changes of NiO–YSZ electro-catalytic electrode. The electrochemical reactor with multi-layer electrode should operate much lower operating voltage and temperature for an effective NO decomposition in the presence of excess oxygen.

Acknowledgements This work has been supported by METI, Japan, as part of the Synergy Ceramics Project. Part of the work has been supported by NEDO. The authors are members of the Joint Research Consortium of Synergy Ceramics.

References

1) Lerdau, M. T., Munger, J. W. and Jacob, D. J., *Science*, Vol. 289, pp. 2291-2293 (2000).
2) Finlayson-Pitts, B. J. and Pitts Jr., J. N., *Science*, Vol. 276, pp. 1045-1051 (1997).
3) Pancharatnam, S., Huggins, R. A. and Mason, D. M., *J. Electrochem. Soc.*, Vol. 122, pp. 1067-1075 (1975).
4) Gur, T. M. and Huggins, R. A., *J. Electrochem. Soc.*, Vol. 126, pp. 869-875 (1979).
5) Hibino, T., *Chem. Lett.*, Vol. 5, pp. 927-931 (1994).
6) Nakatani, J., Ozeki, Y., Sakamoto, K. and Iwayama, K., *Chem. Lett.*, Vol. 4, pp. 315-319 (1996).
7) Washman, E. D., Jayaweera, P., Krishnan, G. and Sanjurjo, A., *Solid State Ionics*, Vol. 136-137, pp. 775-782 (2000).
8) Bredikhin, S., Maeda, K. and Awano, M., *Journal of Ionics*, Vol. 7, pp. 109-115 (2001).
9) Bredikhin, S., Maeda, K. and Awano, M., *Solid State Ionics*, Vol. 144, pp. 1-9 (2001).
10) Bredikhin, S., Maeda, K. and Awano, M., *J. Electrochem. Soc.*, Vol. 148, pp. D133-D138 (2001).
11) Matsuda, K., Bredikhin, S., Maeda, K. and Awano, M., *Solid State Ionics*, Vol. 156, pp. 223-231 (2003).
12) Matsuda, K., Bredikhin, S., Maeda, K. and Awano, M., *J. Am. Ceram. Soc.*, Vol. 86, pp. 1155-1158 (2003).
13) Bredikhin, S., Matsuda, K., Maeda, K. and Awano, M., *Solid State Ionics*, Vol. 149, pp. 327-333 (2002).
14) Lindsay, R., Theobald, A., Gießel, T., Schaff, O., Bradshaw, A. M., Booth, N. A. and Woodruff, D. P., *Surface Science*, Vol. 405, pp. L566-L572 (1998).
15) Rickardsson, I., Jönsson, L. and Nyberg, C., *Surface Science*, Vol. 414, pp. 389-395 (1998).